

Modeling and control of a crushing circuit for platinum concentration

Time dynamic modeling and MPC control of a tertiary comminution circuit

Master's thesis in Systems, Control and Mechatronics

MARCUS JOHANSSON

Department of Product and production development
CHALMERS UNIVERSITY OF TECHNOLOGY
Gothenburg, Sweden 2017

MASTER'S THESIS 2017

Modeling and control of a crushing circuit for platinum concentration

Time dynamic modeling and MPC control of a tertiary comminution
circuit

MARCUS JOHANSSON



Department of Product and Production development
Division of Product development
Chalmers Rock Processing Systems
CHALMERS UNIVERSITY OF TECHNOLOGY
Gothenburg, Sweden 2017

Modeling and control of a crushing circuit for platinum concentration
Time dynamic modeling and MPC control of a tertiary comminution circuit
Marcus Johansson

© MARCUS JOHANSSON, 2017.

Supervisor: Chris Steyn, Anglo American Platinum
Ruan Fouchee, Anglo American
Gauti Asbjörnsson, Chalmers, Product and Production development
Erik Hulthén, Chalmers, Product and Production development
Examiner: Magnus Evertsson, Product and Production development

Master's Thesis 2017
Department of Product and Production development
Division of Product development
Chalmers Rock Processing Systems
Chalmers University of Technology
SE-412 96 Gothenburg
Telephone +46 31 772 1000

Cover: The MPC controller embedded block in the simulation, the zone structure used in the HPGR model and a panoramic view of the dry processing section at Mogalakwena North Concentrator.

Typeset in L^AT_EX
Printed by REPROSERVICE
Gothenburg, Sweden 2017

Modeling and control of a crushing circuit for platinum concentration
Time dynamic modeling and MPC control of a tertiary comminution circuit
MARCUS JOHANSSON
Department of Product and Production development
Chalmers University of Technology

Abstract

In the platinum rich country of South Africa, the British and South African registered company Anglo American operates a platinum mine, this specific platinum mine, the Mogalakwena mine is the worlds largest platinum mine. The blasted ore from the mine pit is processed through a series of crushing and milling stages. This master's thesis work have aimed to time dynamically model and control one of these stages, namely the tertiary crushing stage. This circuit includes an HPGR crusher closed with screens. A time dynamic model of the crusher and the circuit has been built. The tertiary circuit have thereafter been calibrated and validated in this work. A simulink model of the process has been built and used for testing the performance of the circuit, using both the current control setup and a newly developed MPC controller utilizing the FORCES Pro solver in MATLAB simulink. The simulations indicate a potential upside in circuit performance to be achieved either by the change of screen decks or introducing a new supervisory controller and increasing the allowed tonnages.

Keywords: HPGR, Comminution, time dynamic modeling, MPC, Process control

Acknowledgements

The work with this thesis has been an adventure for me and I have truly enjoyed every minute of it. I'd like to express my appreciation to my examiner and supervisor Prof. Magnus Evertsson for making this project possible and all the great discussions regarding the work. I'd also like to thank Dr. Gauti Asbjörnsson and Dr. Erik Hulthén for their support. In addition thank you to all colleagues in the Chalmers Rock Processing Systems Research Group.

During my time in South Africa both at site and in Johannesburg I had very good support from Herman Kemp, Mashudu Munyai, Nthabiseng Tsuke and Felix Kekana at the Mogalakwena mine and in Johannesburg a big thanks to Chris Steyn, Ruan Fouchee, Johan van Rooyen and Jens Lichter for their support of the project and helping out.

I'd also like to express my gratitude to the Anglo American center for sustainable comminution for funding the project via the Global Comminution Collaborative.

Marcus Johansson, Gothenburg, June 2017

Contents

List of Figures	xi
List of Tables	xv
Abbreviations	xvii
1 Introduction	1
1.1 Context	2
1.2 Objectives/ Problem	2
1.3 Research questions	2
1.4 Research approach	3
1.5 Structure of Thesis	4
2 Background	5
2.1 Crushing at Mogalakwena North	5
2.1.1 Primary crushing	5
2.1.2 Secondary crushing	6
2.1.3 Tertiary crushing	8
2.2 Time dynamic modeling	11
2.2.1 The HPGR crusher	11
2.3 Control models	11
3 Methods	15
3.1 Circuit modeling	15
3.1.1 Prerequisites	15
3.1.2 Conveyors and feeders	16
3.1.3 Silos and bins	17
3.1.3.1 Silo 406	17
3.1.3.2 HPGR feed bin and screen bin	18
3.1.4 Screens	19
3.1.5 High Pressure grinding rolls crusher	19
3.1.5.1 The model structure	20
3.1.5.2 Crusher dynamics	20
3.1.5.3 Particle size prediction	24
3.1.6 Model assembly	24
3.1.7 Model calibration and validation	25
3.2 Controller development	27

3.2.1	SISO control layer	27
3.2.2	MPC development	30
3.2.2.1	The process model	31
3.3	Model and controller evaluation	33
3.3.1	SISO Layered control	33
3.3.2	MPC based supervisory control	33
4	Results	35
4.1	Model performance	35
4.2	Current control layer	37
4.3	MPC controller performance	41
4.4	Evaluation of circuit changes	45
4.4.1	Using the current control setup	45
4.4.2	Using the MPC	46
4.4.3	Comparing the two controllers	46
5	Conclusion	49
5.1	The research questions	49
5.1.1	Research question 1	49
5.1.2	Research question 2	50
5.1.3	Research question 3	50
5.2	Discussion	51
5.3	Future work	52
	Bibliography	53
A	Pressure response experiments	I
A.1	Presentation of the pressure response results for the Mogalakwena ore.	I
B	MPC setup	III
B.1	Control model	III
B.2	Control objective and tuning	III
C	Model calibration Figures	V
C.1	Training dataset and validation set	V
D	Process layouts	XV
D.1	Process layout illustrations	XV

List of Figures

1.1	Schematic view of section 406 at Mogalakwena North concentrator. The read markers are the positions of mass flow sensors throughout the section.	3
2.1	Schematic view of the dry section at Mogalakwena North concentrator, including the equipment and the weightometer sensors in red. . .	6
2.2	The primary stockpile at MNC and in the far background on the right the gyratory crusher is located.	7
2.3	The secondary crusher bin, with fresh feed coming from the left and circulated material from the right, the crushers are located on the rear side of the bin.	7
2.4	The feeding chute of the HPGR crusher in gray and the OMAR gates enclosed by the blue structure.	9
2.5	The left side of the HPGRs hydraulic system, showing the red plunger cylinders.	10
2.6	A drawing of an HPGR crusher based on the FLSmith design, by J. Quist [26]	12
2.7	The basic scheme in MPC, by M. Behrendt	13
3.1	Example of a feeder rate in % of maximum belt speed plotted against feeder output for a 8h dataset, where the red line is the least squares fit of a straight line to the data.	17
3.2	Illustration of the structure used for the two silos.	18
3.3	Illustration of the bin structure used for the HPGR and the Screen bin, The striped areas illustrate the active volumes, observe that the illustration is not to scale.	19
3.4	The model structure used in the HPGR block in the simulation model.	20
3.5	a) forces in the x-direction acting on the floating roller, b) a symmetric pressure distribution resulting in a distributed load on the floating roller, seen from above.	21
3.6	a) The zone structure of the HPGR model, b) the hydraulic cylinder setup and the introduced spring damper component. p_h and D_p are the hydraulic pressure and the plunger cylinder diameter respectively.	22
3.7	Left: example of an exponential function fitted to compression data from a Piston and die laboratory test.	23
3.8	A reduction step of a feed and the resulting product for the reduction used by the crusher.	25

3.9	Schematic view of the current control setup used at section 406, consisting of PID-loops and an advanced controller on the screen feeders.	27
3.10	The split of the geometries defining the bed. Left is the approximated shape of the conveyor profile and to the right the two geometries separated. The distance b is the arc length of the circle segment. . . .	29
3.11	The graphical illustration of the state space model used in the MPC controller, The full sized figure is also available in Appendix D	33
4.1	The model response for the circuit production with dataset 1, illustrating the result on the output of a empty screen bin during the time intervals when the model prediction is oscillating.	36
4.2	The production rate of the circuit over an 8-hour simulation with the current control layer.	38
4.3	(Left) the HPGR throughput and the control signal. (Right) The level in the HPGR bin.	38
4.4	(Left) The resulting control signals for the two screen feeders. (Right) The level in the screen bin.	39
4.5	Inflow to the circuit and the circulating load for an 8-hour simulation with the current control setup.	40
4.6	The chute weight for an 8-hour simulation.	40
4.7	The result of the using an MPC to regulate the process, when maximizing output on the product belt CV007	42
4.8	(Left) HPGR crusher throughput and (Right) HPGR bin level	42
4.9	(Left) Screen throughput and (Right) Screen bin level	43
4.10	The inflow into the circuit from the 406 silo.	44
4.11	Solver time for the controller, the beginning of the simulation the controller may have some problems to find feasible solutions to the control problem.	44
4.12	The weight of the chute during an 8 hour simulation with the MPC controller.	45
4.13	Simulation results from 4 different screen apertures for both a startup sequence and a steady state sequence.	46
4.14	Simulation results from 4 different screen apertures for both a startup sequence and a steady state sequence using the newly developed MPC controller.	47
4.15	Simulation results from 4 different screen apertures for both a startup sequence and a steady state sequence using the current control system.	47
A.1	Resulting pressure responses for all size distributions tested.	II
A.2	Particle size distributions used for the compression tests.	II
B.1	The A and B matrices where the non zero entries are visualized with a blue dot.	III
C.1	HPGR production, WIT402	VI
C.2	Circulating load, WIT416	VII
C.3	Circuit inflow, WIT010B	VIII

C.4	Circuit output, WIT433	IX
C.5	HPGR-bin level, LIT100/101	X
C.6	Screen-bin level, LIT405/406	XI
C.7	HPGR predicted capacity	XII
C.8	HPGR operating Gap	XIII
D.1	Section 406 at Mogalakwena North.	XVI
D.2	SISO loops on section 406 at Mogalakwena North.	XVII
D.3	The control model used in the MPC controller.	XVIII

List of Tables

3.1	The parameters of the PID-loops on section 406 both the ones used in the model and on the actual plant.	29
3.2	A list of the considered MV's and CV's	30
4.1	The NRMSE values of the model compared to the plant data for 4 different data sets, a perfect match between the plant data and the model corresponds to a NRMSE of zero.	36
4.2	The NRMSE values of model correspondence to the plant data for the bins for 4 different data sets	37
A.1	Calibration of the force response model from the material	I

Abbreviations

APC	Advanced Process control
CV	Controlled variable
DEM	Discrete Elements Methods
DMC	Dynamic matrix control
GPC	Generalized Predictive control
HPGR	High Pressure Grinding Rolls
MNC	Mogalakwena North Concentrator
MPC	Model Predictive control
MV	Manipulated variable
NRMSE	Normalized root mean squared error
PGM	Platinum group metals
PLC	Programmable Logic controller
PSD	Particle size distribution
SCADA	Supervisory Control And Data Acquisition
SISO	Single Input Single output
TPH	Tonnes per hour

1

Introduction

Practically all metals used in processes and products today have once been mined and refined, this process takes place in an industry known as minerals processing. Different metals are found in different ores and in various concentrations. In order to harvest the precious metals, the blasted ore needs to be reduced in size and gauge particles removed to increase the concentration of the valuable metal. The industrial process chain for size reduction and concentration is typical of a flow based process industry, where each machine used have different capabilities and are constrained in different ways. This process is costly and in many cases requires processing of large tonnages.

Platinum grouped metals, for short PGM's includes the following metals; ruthenium, rhodium, palladium, osmium, iridium, and platinum, which are all noble metals. The largest known reserve of PGM's is located in the Bushveld Complex in the Limpopo Province in South Africa [16]. The Bushveld complex consist of a three main areas, western, eastern and northern Bushveld, in which the ore is high in platinum concentration. Going north from the town of Mokopane on the northern Bushveld the Platreef is located, a 10-400m thick stream in the ground that holds platinum group metals [16]. The ore body in this area where the platinum is found is sulfur rich and the platinum is said to be contained in the grain boundaries [16]. The concentrator where this work has been carried out lies on the Platreef belt in the Municipal of Mogalakwena. At this location the platinum rich ore is found close enough to the surface making it possible to mine with an open pit, instead of being underground. The open pit mine, Mogalakwena is fully owned by Anglo American and is the largest open pit platinum mine in the world as well as the flagship platinum operation for Anglo American [1]. The platinum concentration the at Mogalakwena is relatively high and combined with the open pit this improves the profitability of mining here. The Mogalakwena complex has two concentrator plants, the South plant and the North plant.

The master's thesis work presented here is focused on processing of platinum ore to refine platinum from the ore body. The background, objective and structure of the work will be presented in this chapter. A general view of the subject is presented in the background chapter.

1.1 Context

In process industry where large amounts of materials has to go through the process every hour equipment of high standards and of adequate size is required. The Mogalakwena North Concentrator is the largest and one of the most important for Anglo American Platinum and the success of this top asset is very important for the company [1]. The performance of the plant is top priority and downtime is very costly. The plant is designed in a single stream fashion, implying that there are many sections of the plant where every piece of ore has to go through. There are advantages and disadvantages to this type of plant structure, one advantage is the usage of large scale efficient equipment, on the other hand a disadvantage is the sensitivity to equipment failure. The later has been addressed by large silos in between each section of the plant, enabling some buffer time for the neighboring section in the case of a breakdown.

Considering the above facts a way to test new circuit configurations and control strategies and study the response over time without impacting the production can be a very useful tool. A tool of this sort was built by Asbjörnsson [2] for the secondary crushing circuit, section 405 at Mogalakwena North and the usage of it has been successful for Anglo American Platinum, especially on the control side.

1.2 Objectives/ Problem

Anglo American suggested that a similar model to the one previously built for section 405 to be developed for the next section, the HPGR- circuit , shown in Figure 1.1. The model should represent the circuit in its current configuration and fulfill the below listed requirements.

- Model prediction $\pm 10\%$ of the logged plant data
- Inclusion of silos before and after HPGR-section
- Build the local control loops used today

The sub circuit 406 does not today have any advanced controller supervising its operation, however there is a separate setpoint calculation for the screen bin PID's to make sure the screen bin is not in danger of becoming full and the product belt for the HPGR has to stop. An initial exploration of applying model predictive control to the simulation models was also wished for.

1.3 Research questions

Apart from developing and calibrating the model the following questions will be answered in this thesis.

1. What type of model characteristics are required for time dynamic simulations?

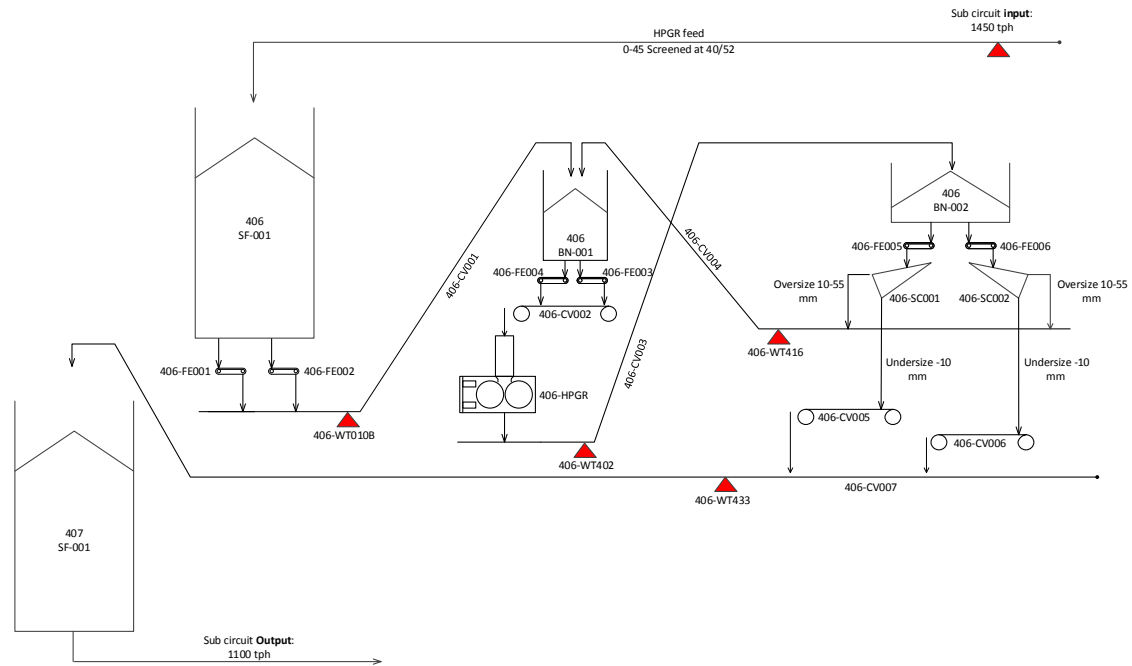


Figure 1.1: Schematic view of section 406 at Mogalakwena North concentrator. The red markers are the positions of mass flow sensors throughout the section.

2. How can large variation and uncertainties in incoming feed and machine wear be handled in order to increase robustness of control system performance?
3. How can model predictive control be applied to a crushing circuit simulation?

Research Question 1 aims to be answered by literature review and during the development of the new model, the confirmation if the new model works is given by the validation. Research Question 2 aims to be answered by the use of simulations with the advanced controller and the development of new controllers. Research Question 3 will be answered by the experience gained by applying model predictive control to the simulation model.

1.4 Research approach

The research approach used in this work is based on a clear definition of the problem, then followed by a literature review to establish a view of what has been done previously in the field. When the current state of the research regarding the problem has been established the list of things which need to be developed is clearer and the work can be structured in an efficient manner.

The work includes a big dependency, which is that the calibrated model needs to be available to test the controller, the controller can be developed before then. However, the model needs to be calibrated before any valid conclusions can be drawn from the use of the controller.

1.5 Structure of Thesis

The thesis is structured in a traditional IMRAD structure beginning with introduction of the subject, then followed by a detailed description of the methods used to solve the task and answer the research questions. Each section will be divided into modeling related and control related topics. This split will follow through the entire thesis. The results of the modeling and calibration are then presented in the results section followed by the performance of the controllers. Conclusions will be given in Chapter 5 followed by answers to the research questions. A discussion is then held regarding the work presented in this master's thesis and brief outlook into the future is also given.

2

Background

A brief description of the process at Mogalakwena North is described in this chapter, followed by an introduction of time dynamic modeling, finally giving some background on the suggested control strategies to be used in this work along with the time dynamic model.

2.1 Crushing at Mogalakwena North

Minerals and metals are found by exploration of new lands and where rock core samples are taken and analyzed. If minerals of value are found extraction can start. The process of extraction usually starts with blasting, regardless if it is open pit or under ground. The blasted ore body usually consists of a wide size range of particles. To extract the metallic minerals, the ore has to be concentrated. Depending on the concentration in the original ore the concentration process varies slightly. At Mogalakwena, and at platinum mines, in general, the concentration of platinum is very low. When a newly commissioned mine opened on the farm next to the Mogalakwena mine complex the platinum concentration was estimated to 1.889 grams of platinum per metric ton of ore [35] in 2015. Platinum is found sprayed in the ore body in very fine grains and requires a large reduction in size applying fine grinding to an average particle size (by weight) of about $7 \mu m$ [10]. Achieving this size reduction is a heavy job and requires large machines and energy. This process is referred to as comminution [37]. A typical plant is divided into dry and wet processing, this thesis will only handle dry processing and therefore in this case only include comminution. The topics described in 2.1.1, 2.1.2 and 2.1.3 are referred to as crushing, at Mogalakwena North the HPGR crusher is both a tertiary and quaternary crusher and will be the focus of this work.

In Figure 2.1 the dry section is illustrated, block a) featuring the primary crusher referred to as section 401, block b) the secondary crushers and section 405 and block c), the HPGR circuit called section 406. Each of the blocks will be described more in detail in this section.

2.1.1 Primary crushing

Primary crushing is done with a crusher that has a large intake and can handle rock particles of sizes up to a couple of meters. At MNC a large gyratory crusher is used to complete the first reduction step in open circuit. An open circuit is implying

2. Background

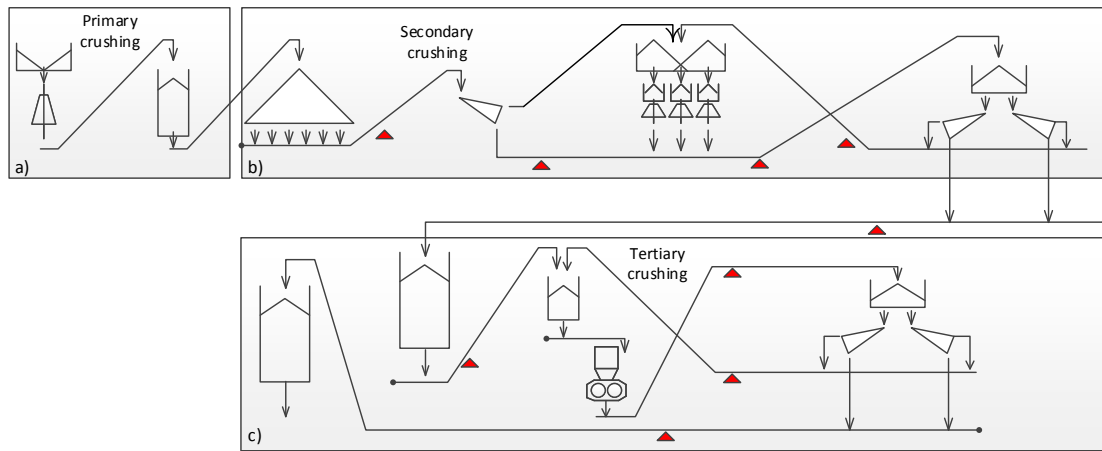


Figure 2.1: Schematic view of the dry section at Mogalakwena North concentrator, including the equipment and the weightometer sensors in red.

that there is no circulation of material back to the crusher. The ore is after that transported on conveyors to the stockpile. The stockpile is pictured in Figure 2.2.

2.1.2 Secondary crushing

The secondary crushing of the ore is achieved with cone crushers. A cone crusher can handle a large variety of feed sizes, in this case ranging from 360 mm and down. At Mogalakwena North three cone crushers are used in a closed circuit with screens. The first two crushers are crushing mainly fresh feed from the primary crusher and the third crusher the circulated $+55[mm]$ material. The product from the cone crushers is then screened and transported to the HPGR-fresh feed silo. The secondary crushing section is today controlled by a controller developed with the help of the previously developed time dynamic simulation model by Asbjörnsson [2] and validated by Brown and Steyn [27]. The secondary crusher lineup consists of a three Hydrocone H8000 made by Sandvik. The crushers have a large capacity, and the current operating point of the plant allows for the use of two crushers at the time. This set up is beneficial for the plant and the crushers, if crusher one and three are used, this will create a wall between the crushers and separates the circulating load from the fresh feed. The secondary circuit is today supplying the HPGR section, box c) in Figure 2.1, with a material screened at 55 by 55 mm screen decks.



Figure 2.2: The primary stockpile at MNC and in the far background on the right the gyratory crusher is located.



Figure 2.3: The secondary crusher bin, with fresh feed coming from the left and circulated material from the right, the crushers are located on the rear side of the bin.

2.1.3 Tertiary crushing

The final sub circuit on the dry side of the process is the HPGR section also referred to as section 406. This section is modeled, simulated and controlled in this work. The section houses a ThyssenKrupp Polycom 16/22 high pressure grinding rolls crusher or HPGR crusher for short. The product from the secondary crusher circuit is stored in a silo and is fed to the HPGR-bin where it is combined with the oversize from the screens. The HPGR bin is equipped with two variable speed drive feeders which are feeding onto a variable speed belt. The HPGR crusher should be running in choke fed conditions, implying there should always be material in the chute above the crusher. The chute is hanging in load cells, which measures the weight of the chute. The chute is pictured in Figure 2.4. The HPGR has been upgraded from the original commissioning of the plant, now having larger motors driving the rolls, which also features variable speed drives on the rollers. The original set up of the HPGR circuit is described by Rule [29] in a paper written after the commissioning of the plant in 2008. The product of the HPGR is transported to the tertiary screens with apertures of 10 by 10 mm to date. The oversize is conveyed back to the HPGR bin, and the passing material goes into two silos supplying material into the wet process and the primary mills.

The HPGR crusher crushes the ore by passing it between two pre-tensioned rollers, in this case, pressurized with 160 bar hydraulic pressure with active pressure and dampening control. Each side of the crusher has two plunger cylinders, and a controller is actively differentiating the pressure between the two sides to keep the gap constant between the two rollers over the entire width of the rolls. The left side (seen from above) of the machine the hydraulic cylinders are shown in Figure 2.5. The hydraulic system is protected by two nitrogen accumulators, one on each side of the machine, these are installed to minimize the effect of high-pressure spikes, which can appear in hydraulic systems. The hydraulic system is also equipped with an active dampening controller to protect the machine in case of tramp metal or overload.



Figure 2.4: The feeding chute of the HPGR crusher in gray and the OMAR gates enclosed by the blue structure.



Figure 2.5: The left side of the HPGRs hydraulic system, showing the red plunger cylinders.

2.2 Time dynamic modeling

Time dynamic modeling aims to describe how a technical system changes over time. It ranges from being the solution to the differential equation that describes how an object free falls to the state of a process industry. The applications of dynamic modeling are many and are usually related to, physics, chemistry, control, mathematics or other technical fields where there is a need to describe time dependent and varying processes. In comminution the topic is introduced in [31], outlining the basics of modeling comminution circuits, much similar to the approach by [2]. The first dynamic models and approaches of describing comminution over time have been done within milling, to mention a few: Liu [18], Salazar [30] and Rajamani [28] where the more recent ones utilized a Simulink environment for the simulation as suggested in [31] and by Asbjörnsson [2]. The modeling work done by Asbjörnsson at Mogalakwena North on the secondary crushing circuit developed a few common components which can be used for the HPGR-section as well, these include conveyors, screens, and bin-structure. The remaining component, the HPGR-crusher has been developed in this work. State of the art in HPGR crusher modeling will be reported upon in Section 3.1.5.

2.2.1 The HPGR crusher

The development of the HPGR crusher can be related to the work done by Klaus Schönert on breakage mode of rock and applying his results [32], [33]. Schönert concluded that single particle breakage is the most effective mode of breakage and the second most effective breakage mode, regarding energy, is confined bed breakage. To achieve the bed breakage mode, a conventional roller crusher was fitted with hydraulic cylinders to increase the pre-tensioning between the rollers.

The HPGR first established itself as a crusher in the cement industry in the 1990s, later spreading into minerals processing applications [22]. The potential of the crusher in the minerals processing industry have been highlighted by multiple authors, Rule [29], Ntsele [24] and Powell [25]. A schematic view of the crusher is shown in Figure 2.6. The crushed ore is compressed to the extent that the formation of cakes appears in the product, these cakes are brittle and include micro cracked rocks [37], that in most cases will separate into very fine particles once shaken on a screen or from the fall into the bin in hard rock application similar to MNC [22].

2.3 Control models

Large scale processes with machines that have different operational windows and parameters need control to function correctly. Control is implemented for multiple reasons, for example to stabilize and achieve a smooth operation, to protect the equipment and to ensure the process product maintains a certain quality. Stabilizing control is implemented at MNC as a layer of single input single output (SISO) control loops running on a programmable logic controller (PLC) . This computer handles the protective part of the control and allows for basic stable operation, discrete logic

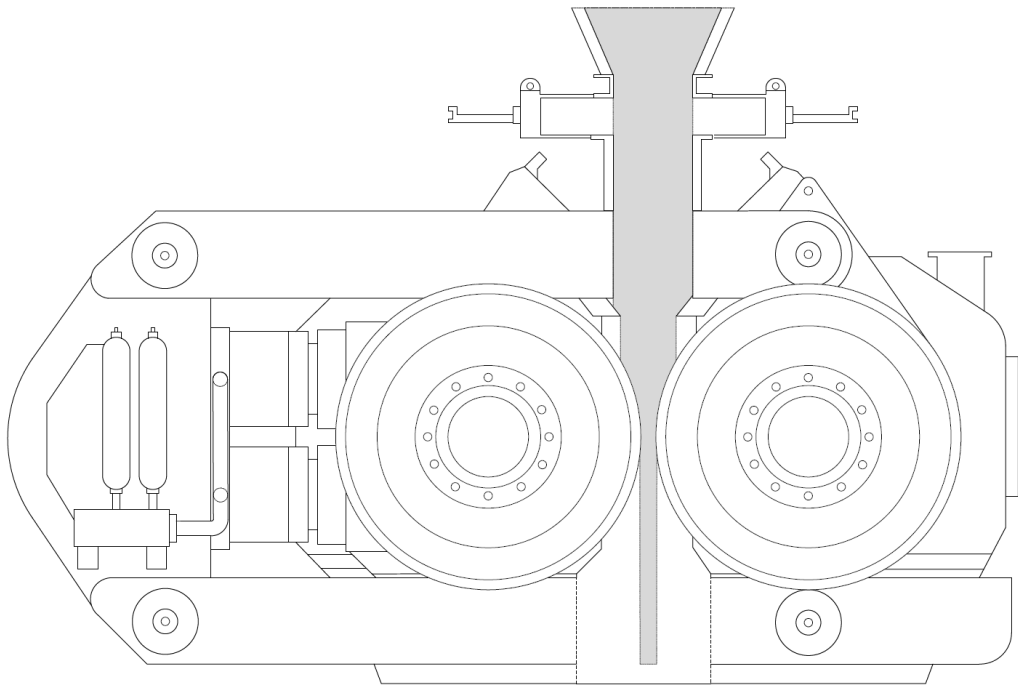


Figure 2.6: A drawing of an HPGR crusher based on the FLSmidth design, by J. Quist [26]

and start up sequences are also included in this layer. The common practice in the industry is described by Tatjewski [36]. On top of this basic control layer, there is a possibility to add more advanced controllers, typical supplying the set points, or references to the basic layer.

The types of controllers used for optimizing and balancing on a higher level than the SISO loops are usually grouped into advanced controllers. One of the best established and very powerful type of controller, in process control, is the model predictive control scheme or MPC for short. The predecessor to MPC was developed in the Petrochemical industry at the end of the 1970s. This type of controller is called dynamic matrix control (DMC) controller and uses step response models to predict the future state of the process. Cutler and Ramaker [11] introduced this scheme at the Shell refinery in Houston, Texas. The basic idea was to use the step response models to predict the future of the process and choose the control signals or set points optimally. The first approach was slightly primitive and couldn't handle constraints very well. Increases in computational power have successively increased the capabilities of the scheme and to approach more advanced problems. DMC evolved to generalized predictive control (GPC) and finally to MPC which is the common form today. MPC software is readily available for businesses to buy and apply to their processes. A summary of MPC controller development and an outlook into the future is given by Morari [21]. Outlining the future regarding more complex models, constraint handling, and robustness. Model predictive control has with more computational power the ability to solve control problems with very demanding time requirements.

In Figure 2.7 a reference trajectory, the red line is to be followed, the MPC algorithm, based on a cost function, will calculate a set of control inputs up until time $k + p$, at time k the first of the control inputs is applied to the process and the optimization is carried out again at time $k + 1$. In the objective, the control inputs that minimizes the difference between the reference and the predicted output, the brown line in Figure 2.7 is calculated.

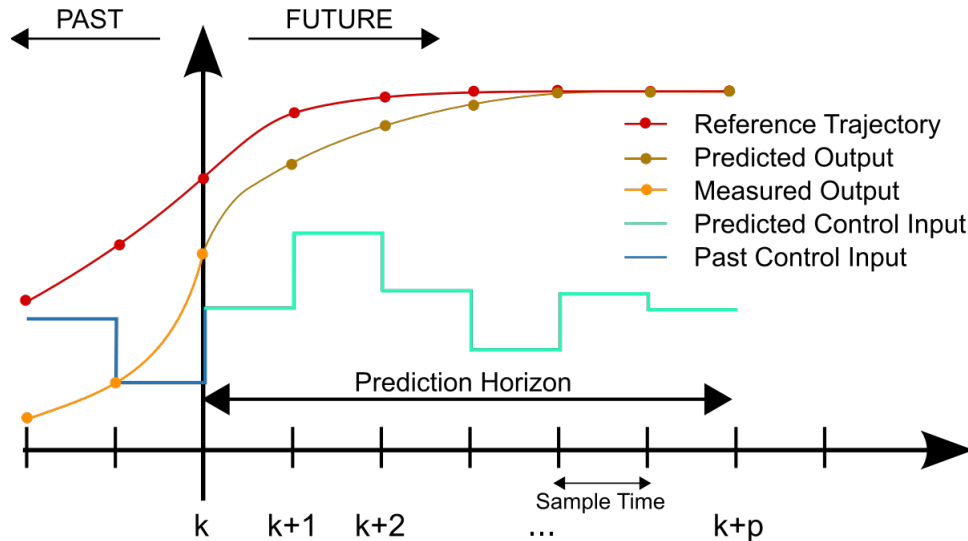


Figure 2.7: The basic scheme in MPC, by M. Behrendt

This type of controller is optimal in regards to the model used in the calculation of the output prediction. There are many ways of describing the models used in the controller, two of the most common are; step response models and state space models. Step response models are common in the industry, and state space is usually the choice of researchers when developing new algorithms. This work will utilize state space models since those are easily used in Simulink in connection with the model.

3

Methods

The following chapter will be divided into modeling and control where the modeling techniques will be discussed first then followed by the controller development.

The task of modeling section 406 can be divided into two different types of work, modeling related and calibration or tuning related. The modeling work includes the following:

- HPGR crusher model
- Silo models
- Bin models
- Conveyor

The above has to be developed from the ground or largely modified from previous work by Asbjörnsson. The most important of the above is the HPGR model, as described in Section 2.1.3.

The second task, the calibration of the model needs to be done to make sure the model corresponds to the process itself. Calibration includes: Balancing the mass flow in and out, Particle size prediction and bin levels within the circuit.

3.1 Circuit modeling

The first aim of the master thesis project was as described in Section 1.2 to model the HPGR section at the Mogalakwena North Concentrator. The approach to how this is done is described in this section along with explanations to how the material handling equipment and screens are modeled.

A set of requirements for the final model was also formulated by Anglo American Platinum and are listed in Section 1.2.

3.1.1 Prerequisites

In each sampling instant at every point, the circuit has a certain mass flow which has a set of properties and a particle size distribution. To track particle size, mass flow and properties of the material, a data structure is needed to specify what information should follow with each time step of the model. The introduction of the structure used in this work was done by Asbjörnsson, [2]. This was done to facilitate the connection of the model of the secondary crushers to the one being developed

in this work. The modeling work was therefore done in MATLAB Simulink of compatibility reasons.

3.1.2 Conveyors and feeders

Section 406 has two different types of conveyors and one type of feeders. The two types of conveyors are fixed speed conveyor and variable speed conveyor. All conveyors are fixed speed except **406CV002**, which is the conveyor feeding into the HPGR-chute. This conveyor can speed up or down depending on the weight of the chute to ensure the HPGR crusher stays choke fed. All feeders are equipped with variable speed drives to adjust the output of the feeder. The conveyor models are described by Asbjörnsson in [4] and [2].

A regular fixed speed conveyor introduces a delay in the process; this is modeled as a pure delay, using standard Simulink blocks for delaying a signal. The time delay can be expressed with Equation 3.1

$$t_{delay} = \frac{L_{conveyor}}{v_{conveyor}} \quad (3.1)$$

where L and v are the length and speed of the conveyor.

The variable speed conveyor is modeled with a state space that keeps track of the material on the conveyor as a function of conveyor length. This conveyor model allows for stopping the conveyor without losing any mass, which is the case with the fixed speed conveyor.

On section 406 there are six variable belt feeders, pulling material out off the bins and silos on the section. These are controlled with PID-loops supplying the feeder with a percentage of its maximum belt speed. Since all feeders have weightometers close to them, the corresponding material being fed to the process for a specific value of the feeder control signal can be plotted. The output of the feeders is approximated to be linear with belt speed. A straight line was fitted for each of the feeders. In Figure 3.1 the relationship between the feeders **406FE001** and **406FE002** combined against the mass flow recorded on weightometer **406WIT010B**. The same method was used for feeder **406FE003**, **406FE004**, **406FE005** and **406FE006** as an initial measure. The feeder output model is based on Equation 3.2. Since the feeder model includes two parameters to be tuned, the correct response has to be obtained from more than a single operating point to make sure the rate and the offset are in parity with the real process. Based on this reasoning the feeder rates were estimated from all training datasets and averaged. The offset term in the linear equation was kept fixed to an initial guess and the rate used to calculate a rough estimate. These averages were then used in the first iteration of the model calibration.

$$y = kx + m \quad (3.2)$$

The output y of the feeder was formulated in the form of Equation 3.2. The feeder model includes no time delay, even if there is some delay in the feeder, especially during startups and if the bin or silo have been empty.

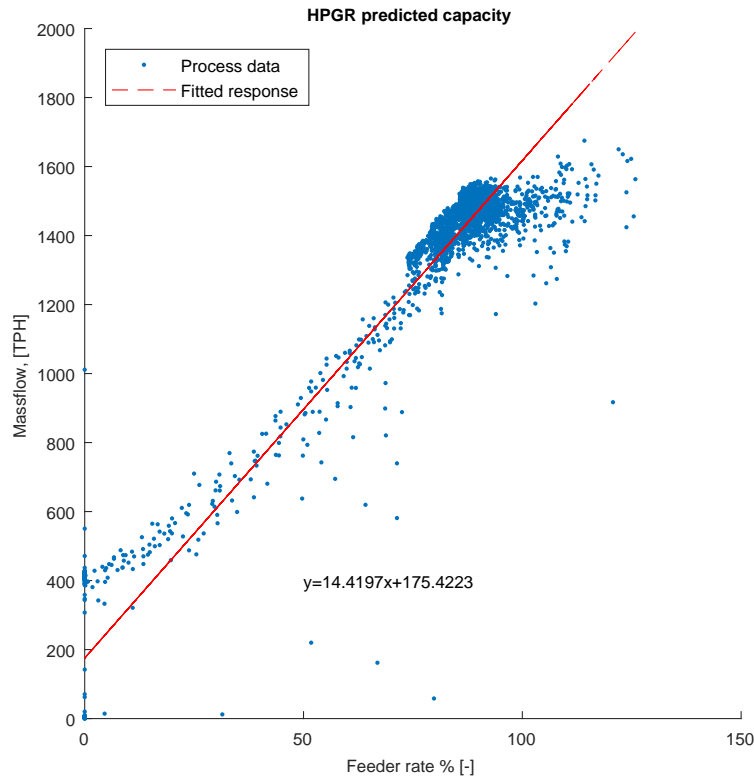


Figure 3.1: Example of a feeder rate in % of maximum belt speed plotted against feeder output for a 8h dataset, where the red line is the least squares fit of a straight line to the data.

A possible extension to this model would be to include a non-linear term saturating the output which can be seen in some instances, as in Figure 3.1 and implement a check if there is enough material in the bin to utilize the entire feeder capacity. This was implemented on the inflow to the circuit, **FE001** and **FE002**.

3.1.3 Silos and bins

The circuit 406 includes three different bins and silos. Modeling of the two smaller bins has been based on Asbjörnsson's bin model presented in [3]. Modeling of each of the three different material storage containers will be described below.

3.1.3.1 Silo 406

The silo storing the secondary product is a 10 000 ton silo, and due to its size, it has been modeled as a layered bin, as shown in Figure 3.2. The silo has been divided into 100 layers, the material is mixed within each layer, resulting in one particle size distribution, one set of properties and a total mass for each layer. The first material to enter the bin is the first to exit, in other words, when the bottom layer has been emptied the layer above will be used, the material is successively moved downwards in the zone structure as indicated in Figure 3.2.

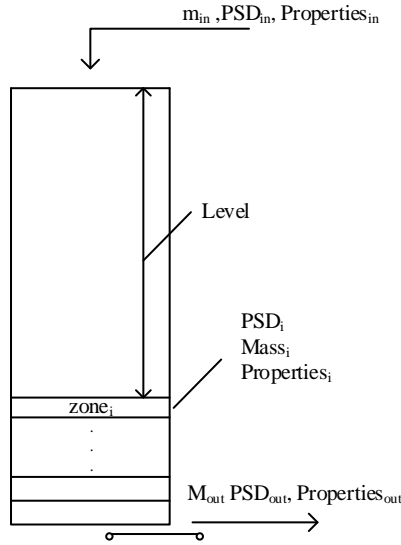


Figure 3.2: Illustration of the structure used for the two silos.

3.1.3.2 HPGR feed bin and screen bin

The two smaller bins on section 406 are the HPGR feed bin and the screen bin, these were modeled with a structure introduced by Asbjörnsson [3]. The two bins are pictured in Figure 3.3, where they work with an active volume, illustrated by the striped pattern. Both bins were assumed to have sections, these sections each have a volume. The middle section receives the incoming material, and the two outer sections are from where the material is withdrawn. Depending on the levels in each section material is transferred between the sections. The transfer and when have been partly calibrated, however, it is a very difficult task and have been second to the mass flow calibration.

The angle between the each of the sections noted $\alpha_{1,2}$ is what determines the transfer, if this angle is larger than the repose angle of the bulk material, transfer between the sections is taking place. Equation 3.3 is the underlying calculation done to determine the transfer, δy is the difference in height between the outer section and the middle section and δx is the distance between the center of the bin and the center of the feeder. This distance is constant since the feeder has a fixed position in the bin. The two outer sections have been modeled with a nonlinear shape in the bottom. They have therefore a shape, as illustrated in Figure 3.3 with a cone in the bottom. This was a way to be able to empty and refill the bins fast, which can be observed in the process data.

$$\alpha_{transfer} < a_{1,2} = \tan^{-1}\left(\frac{\delta y}{\delta x}\right) \quad (3.3)$$

In each bin, there are level sensors which measure the distance from the sensor to the material level using an echo. These sensors are calibrated and have to be recalibrated over time. The readings are noisy and very sensitive to how the sensor

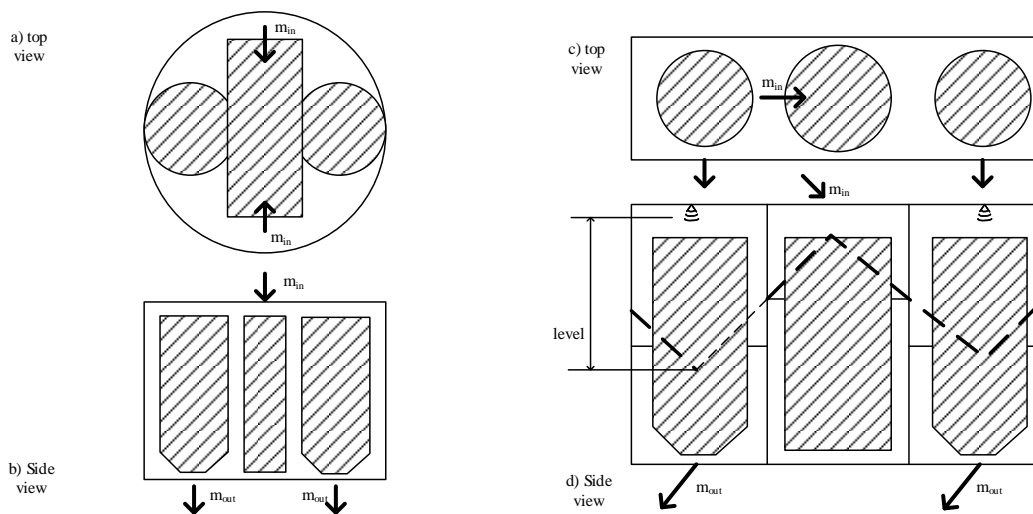


Figure 3.3: Illustration of the bin structure used for the HPGR and the Screen bin, The striped areas illustrate the active volumes, observe that the illustration is not to scale.

is positioned and aimed. The active volume was estimated using process data, however, appeared to vary depending on data set and not in an explainable manner. Apart from the section structure, there is a global first in first out structure on both bins. This structure works as described for the silos in section 3.1

3.1.4 Screens

The model of the two screens **406SC001** and **406SC002** have been the same model as used when modeling was done for section 405 by Asbjörnsson [2]. The only difference is that the aperture of the screens has been set to the size used today, which is a 10 by 10 mm mesh of a polymer material. The screen model originates partly from the work of Staffhammar [34] but have been adapted for use in time dynamic simulations by Asbjörnsson.

3.1.5 High Pressure grinding rolls crusher

The heart of section 406 is the HPGR crusher. This crusher has been subjected to study by many, a summary of the work done on HPGR modeling is given by McIvor [20]. The models to date have been focused on particle size prediction and throughput. Comminution modeling, have in general been focused on steady state simulations and therefor models for the HPGR do not include dynamic components, such as varying gap and roller speed. The closest to the dynamic response is the one that can be observed in DEM-simulations by Barrios [7] and Quist [26]. Where they both have utilized the possibility with the DEM software to feed the forces from the particles to a model describing the hydraulic system. The results are very high fidelity model responses, however, the DEM- calculations are too slow for process simulations. The insights from DEM are very fruitful for the modeling exercise of a

comminution machine.

The most influential models of HPGR's in the literature are based on the Austin roller mill model, first developed for coal [5]. Morrell and Daniel [12], [23] and Benzer [14], [8], have later developed this model with focus on particle size and capacity. The models are more descriptive than predictive, and in a process simulation, predictive and fast models are what is required.

3.1.5.1 The model structure

The HPGR model used for the circuit modeling in this work is based on a new approach, combining mechanistic crusher modeling based on Evertsson's [15] cone crusher model and Johansson's [17] jaw crusher model.

In HPGR modeling, when targeting modeling of the dynamics, multiple approaches have utilized a spring damper system to model the response from the hydraulic system [6] and [26].

The process model developed for this purpose is aimed to capture the dynamics in roller speed changes, pressure, and incoming feed size changes. The model structure used can be seen in Figure 3.4.

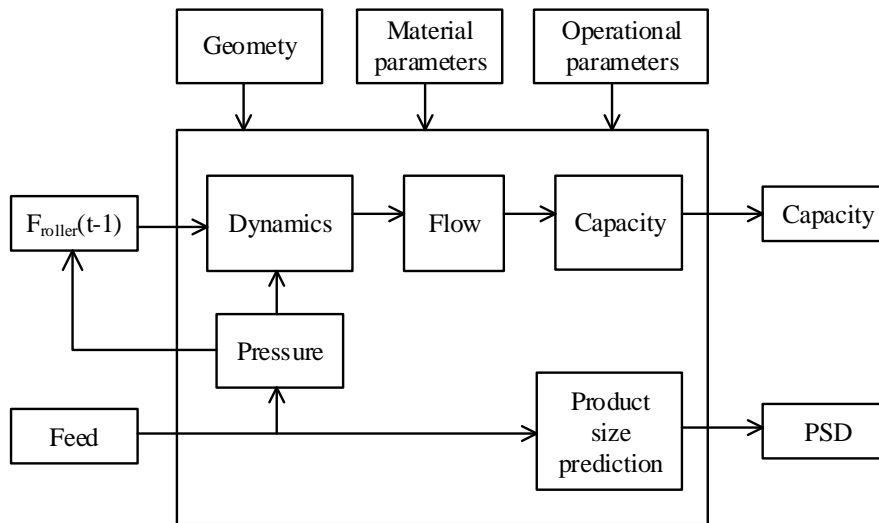


Figure 3.4: The model structure used in the HPGR block in the simulation model.

3.1.5.2 Crusher dynamics

The position of the roller is essential to estimate the throughput of the crusher. To determine the floating roller's position, a free body diagram is completed, and the force balance in the horizontal direction can be stated. In Figure 3.5 a) the free body diagram is drawn, where F_h is the force from the hydraulic system. The hydraulic

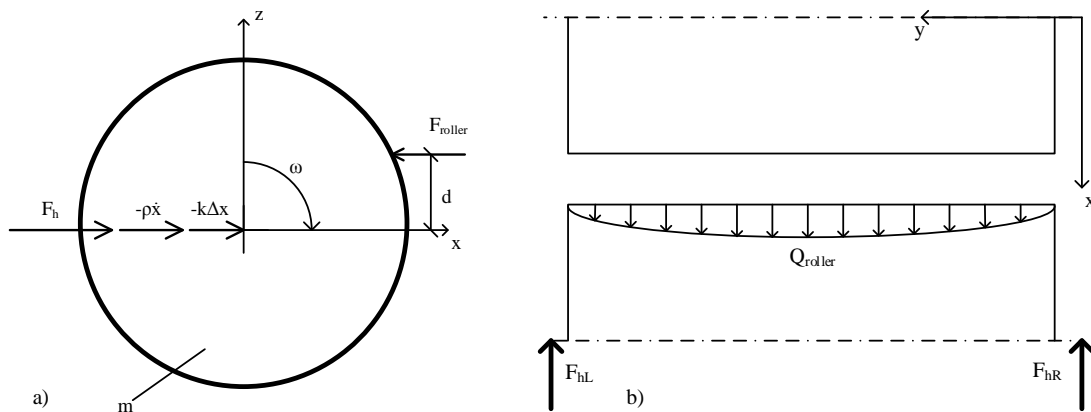


Figure 3.5: a) forces in the x -direction acting on the floating roller, b) a symmetric pressure distribution resulting in a distributed load on the floating roller, seen from above.

system is modeled to have a stiffness and a dampening effect. These forces have been noted as well in the figure. The system is stiff and requires a sampling time much smaller than the one used in the actual process model. The force component from the stiffness is reset in each global sampling instance, implying that Δx is set to zero in each step in the process model's global iteration, the velocity at the final step is used as an initial condition in the next step. F_{roller} is the force from the material because of the compression. The force balance is shown in Equation 3.4, the equation describes the time varying motion of the floating roller, regarding the position, velocity, and acceleration. Equation 3.4 was converted into a state space system for use in the model. The sampling time of the roller equation was set to $400Hz$ in the discrete implementation in the model.

$$m\ddot{x} = F_h + (-\rho\dot{x}) + (-k\Delta x) - F_{roller} \quad (3.4)$$

The component F_h is supplied externally as the hydraulic pressure, F_{roller} is estimated based on a discretization of the compression cycle and over the length of the roller. The hypothesis is that at an angle α , noted in Figure 3.6, and below the boundary condition between the roller and the material bed is assumed to be no slip. The angle α is sectioned in smaller elements α' . The breakage is assumed to be based on pure compression and the position where the material experiences the no slip condition, the distance between the rollers is the distance B , the total compression ratio can be expressed as a function of the operating gap. The relation is shown in Equation 3.5

$$C_{ratio} = \frac{B - gap}{B} \quad (3.5)$$

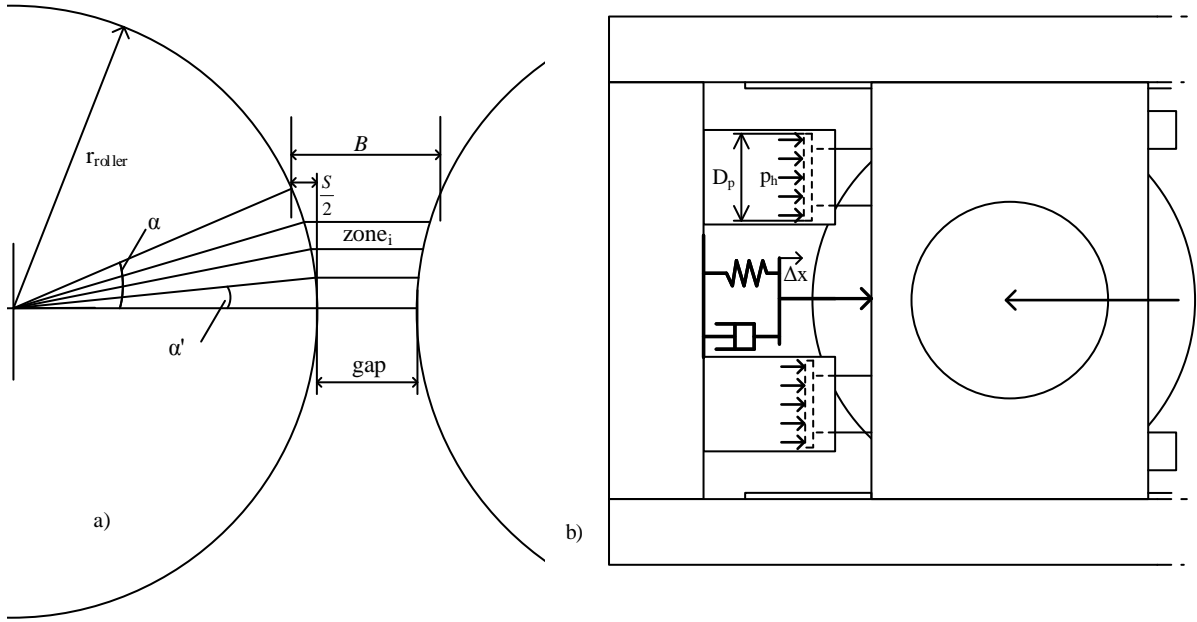


Figure 3.6: a) The zone structure of the HPGR model, b) the hydraulic cylinder setup and the introduced spring damper component. p_h and D_p are the hydraulic pressure and the plunger cylinder diameter respectively.

The throughput of the crusher is calculated as the mass of each zone times the number of zones to pass through the crusher per unit time. The mass of a zone is modeled as the volume of the first zone times the bulk density of the material. If the mass of each zone is saved during the process of compression and assuming no material exits on the sides the total mass over time can be calculated with Equation 3.6

$$\dot{m} = \sum_{j=1}^{n_{zones}} m_{zone_{1,j}}(gap, \alpha') \quad (3.6)$$

From Equation 3.6 it should be noted that $m_{zone_{1,j}}$ is a function of the gap and the angle α' and the number of zones per unit time, n_{zones} is a function of roller speed. The roller speed can be stepwise changed with the global simulation time but stays constant with the smaller steps within the HPGR crusher module. This implies that a re-sampling of the zone structure is done at each global sampling instance.

To determine the force from the material to the roller the feed material at MNC was sampled and compressions test with a piston and die in a hydraulic compression rig were done. The compression rig records the compression ratio along with force during the test, and the results were fitted to an exponential function. The test was done for three different widths of particle size distribution and two different maximum particle sizes. An example of the output from a piston and die of the test is shown in Figure 3.7.

From the test data a double exponential function can be fitted, the fitting was done using MATLAB to fit a function that minimizes the error between the function and

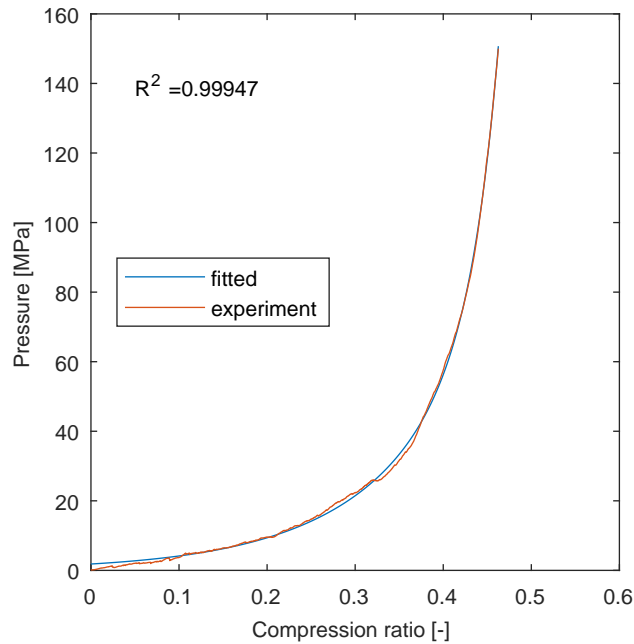


Figure 3.7: Left: example of an exponential function fitted to compression data from a Piston and die laboratory test.

the data in the least squares sense. The function chosen for the pressure response is shown in Equation 3.7. The piston and die tests generated six different force responses depending on the PSD, all results are found in Appendix A.1

$$p = a_1 e^{b_1 x} + a_2 e^{b_2 x} \quad (3.7)$$

To predict the force onto the roller in the no slip compression zone a variable number of zones is used in the z-direction and a fixed number in the y-direction, see Figure 3.5 for the coordinate system. The result is a grid of forces that can be summed into the total force F_{roller} with Equation 3.8.

$$F_{roller} = \sum_{j=1}^{25} \sum_{i=1}^{n_{zones}} F_{i,j} A_{i,j} \quad (3.8)$$

The force is obtained by multiplying the area of each zone by the pressure for the specific compression obtained at the sampling instance. The width of the roller, index j in Equation 3.8, were divided into 25 segments.

In order to arrive at a model simple enough to run in the simulation with the low sampling time and still obtain result faster than in real time the following assumptions are made;

- All loads are symmetric
- The relaxation of the material below the center of the rollers is zero
- The material above the no slip zone does not affect the roller position

In addition the spring damper model uses the following stiffness and dampening, $k = 2 * 10^4 [N/m]$, $\rho = -1000 [Ns/m]$. The mass of the roller arrangement was

estimated to 45 tons. Quist has shown the force distribution along the roller using DEM [26]. For this work, a second order polynomial was used to scale the force along the roller to obtain the maximum force in the middle and lower at the edges. The total response from the compression was tuned to correspond to a gap similar to what the crusher uses in operation. Figure 3.5 b) shows the principle of the load onto the roller, where the polynomial was used to shape the pressure distribution. This loading condition is noted in the literature to vary depending on the HPGR crusher geometry and then specifically if side plates are used. At MNC there are plates on each of the sides of the rollers inhibiting material from escaping.

3.1.5.3 Particle size prediction

The particle size reduction in the crusher is modeled with a fixed reduction and only respond to changes in feed size distribution. The reasoning behind this choice was that the methods used in form conditioned crushing, for example in cone crushers, the particle size distribution behaves very differently compared to in an HPGR. The cone crusher uses a compression ratio based measure as input to the particle size prediction [15]. The method was tested with a model calibrated for an aggregates material, but it was not corresponding well enough to be used in this work. Other methods used in the literature are population balance models which also include many parameters and requires plant surveying. One population balance model by Dundar [14] includes data for a platinum ore. The choice of proceeding with the new model was basically due to simplicity and that the surveys of the plant from 2011 included three different tests with the HPGR and proving it difficult to be conclusive on how to formulate a module to predict based on more inputs than the feed.

The reduction used in the crusher for this model presented in Figure 3.8 The reduction step consists of a vector of values added to the cumulative particle size distribution curve. This action is combined with logic to avoid the distribution to grow larger than 100% as well as from obtaining a negative slope. It should be noted that this model will only work for a narrow range of operation for the Mogalakwena North HPGR crusher and does not aim to describe any other HPGR's crushing performance.

3.1.6 Model assembly

When all the components of the model are available and tested to be in error free state, they can be assembled in Simulink. The main bus consisting of the data structure described in Section 3.1.1 is connected between each component, and the input signals are read from the workspace of MATLAB. Logging of signals was done both by storing them to the workspace as well as graph windows in the model to allow for visual monitoring while running the model. Parameters, such as conveyor belt speeds, inflow feed size, and screen deck apertures were in this process also assigned to the model. Initial testing and debugging were part of the process as well.

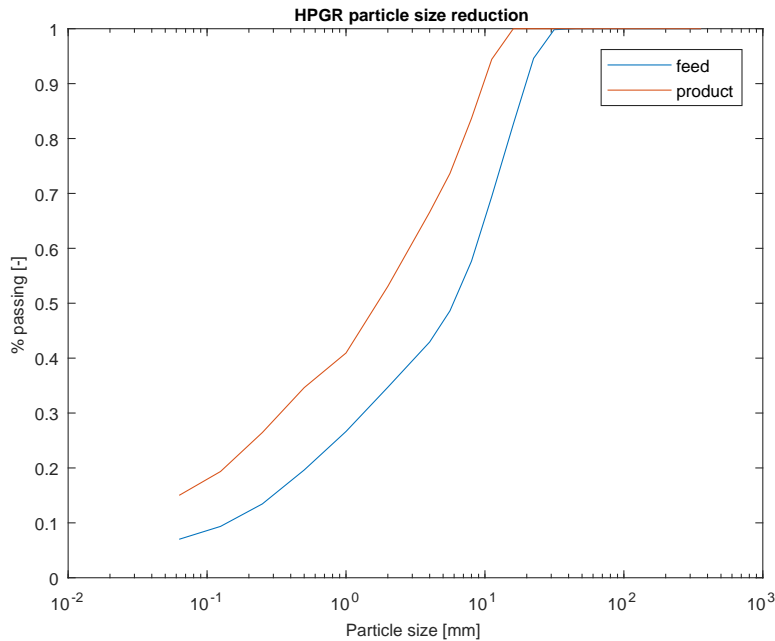


Figure 3.8: A reduction step of a feed and the resulting product for the reduction used by the crusher.

3.1.7 Model calibration and validation

The final model has been calibrated against process data retrieved from the SCADA system at the site. This process was very time consuming, even if the circuit is not complex the effort required to achieve good enough correspondence for many simulations with multiple dataset is large. In this section the work and methods used to achieve the result of a calibrated model will be described.

The validation of the model is based on the work by Steyn and Brown [27] and in summary, the weightometer readings are compared with the model prediction over a number of different datasets. The performance measure of the model used was a normalized root mean squared error, NRMSE, value and the same measure has been used in this work. For each model run of 8 hours Equation 3.9 was used to calculate the normalized error measure between plant data and model prediction. For the calibration of section 406, three different datasets were used and a fourth set for validation. The validation set was picked at random and never used for training of the model.

$$R_{NRMSE} = \frac{\sqrt{\frac{\sum (y - \hat{y})^2}{n}}}{\bar{y}} \quad (3.9)$$

Where y is the measurement from the actual plant, \hat{y} is the model prediction, and n is the number of samples in the eight-hour simulations. This value has been 2881 for all simulations since the SCADA system samples the process every 10 seconds. \bar{y} is the average value of the plant data for the time period. Calibration of other measures than weightometers was done to some extent, focusing on level reading in the two smaller bins, the HPGR-bin, and the screen bin.

To be able to simulate the process using real process data, the SCADA signals were loaded into the model via the MATLAB workspace. It was possible to automate this process which helped to speed up the initialization of the simulations. The calibration used three different datasets and after all had been simulated the results were compiled into a report, and the methods below were used to improve the result for the next iteration of simulations.

The following steps were used to when approaching the task of model calibration with process data. The calibration is an iterative process and the method is usually developed slightly during the completion of the task, the list below resembles the method used towards the end of the task.

1. Identifying three sets of data that the model can capture
2. Mass balance over time, making sure the each feeder output the right amount of mass
3. If more than one feeder per weight sensor make sure the feeders operate equally
 - (a) a. If not determine the ratio between the feeders
4. Estimate the relative bin size or utilized bin size from process data. However, this is just an indicator and depends on the operating point.
5. From all the data sets try to find conclusive trends and reasons to tune parameters.
6. Adjust bin sizes. The trends in the level sensor data from the real plant should be visible.
7. Evaluate performance,
 - (a) If calibrated, proceed to validation else back to 1 and iterate.

3.2 Controller development

The controller development is split up into two parts, firstly to replicate all the local SISO-loops acting on the circuit and to make sure they are stable. After that, an MPC controller was developed and implemented in Simulink. The two parts are discussed separately, however for the MPC controller to be tested the SISO control layer needs to be in place.

3.2.1 SISO control layer

The current configuration of control for the 406 section consists of PID-loops and a setpoint selector for the screen bin. The PID-loops are standard form PI-controllers, where the set-points are supplied either from another loop or fixed. The set point selector for the screen bin is providing set-points to the PID's controllers controlling the screen feeders. The setpoint selector has not been modeled in this work, however, in short, it is making sure the screen bin never becomes full in the case of a stop of any of the belts **406CV004**, **406CV005**, **406CV006** and **406CV007**. This is to protect the crusher product belt from having to stop while in use and loaded. Stopping a fully loaded belt may result in having to empty the entire belt manually before being able to start it again. The effect of not including this controller in the simulation model is discussed in Section 5.2. In Figure 3.9 the control loops are illustrated.

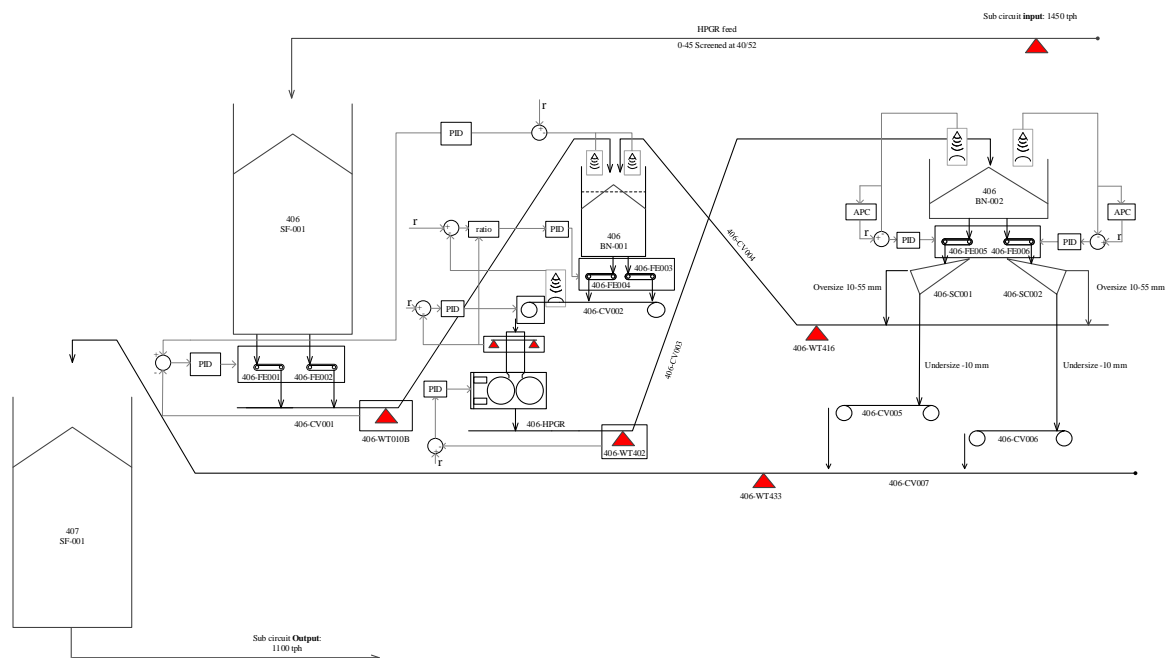


Figure 3.9: Schematic view of the current control setup used at section 406, consisting of PID-loops and an advanced controller on the screen feeders.

The structure is set up with the following goals; to make sure the HPGR is choke fed, no overfilling of bins and that material is always available in the HPGR bin. There is a range of slow and fast control loops on section 406. The PI control loops in use are listed below.

- Feeders from Silo
- Setpoint for Silo feeders
- Feeders from HPGR-bin
- belt speed of HPGR chute belt
- Roller speed of HPGR
- Screen feeders

The feeders that withdraw material from the HPGR bin does that by maintaining a fixed level on the variable speed conveyor **406CV002**. There is a radar sensor above the conveyor that measures the height of the material bed on the conveyor. To be able to do this in the simulation a model describing the filling of the conveyor has to be developed. The derivation follows below.

Every second material is withdrawn from the bin and placed on the conveyor. Since the conveyor speed is updated once a second, the speed during a second is assumed to be constant. If the mass placed onto the conveyor is divided by the bulk density and the distance the conveyor has traveled in one second, the cross sectional area of the conveyor bed is obtained. The conveyor is supported by five rolls which form an arc, the radius of the arc has been estimated to $1.52[m]$ and assuming that the conveyor fills the segment of a circle and creates a 30° angled triangle on top, as illustrated in Figure 3.10. The area of a the circle segment can be calculated with Equation 3.10, 3.11 and 3.12 from Björks [9].

$$A = \frac{1}{2}(br - s(r - h)) \quad (3.10)$$

$$s = 2\sqrt{h(2r - h)} \quad (3.11)$$

$$\sin\alpha = \frac{s}{2r} \quad (3.12)$$

The notation is the same as in Figure 3.10. If Equation 3.10, 3.11 and 3.12 are combined and the area of the triangle is added Equation 3.13 can be stated. This equation is nonlinear and in order to solve for the height h an iterative method was used to for arriving at a value area close to the one calculated based on the mass and the conveyor speed. The iterative approach ramped the height h until it was larger than the reference area. The plant has a set-point for $330[mm]$, and the model predicts a set-point of $380[mm]$ running at the operating point which might indicate that the angle of 30° is too large. However, this was kept the way it is described here.

$$A = 0.5((2\sin^{-1}(\sqrt{h(2r - h)})/r)r^2 - 2\sqrt{h(2r - h)}(r - h)) + \frac{s^2}{2}\tan(30) \quad (3.13)$$

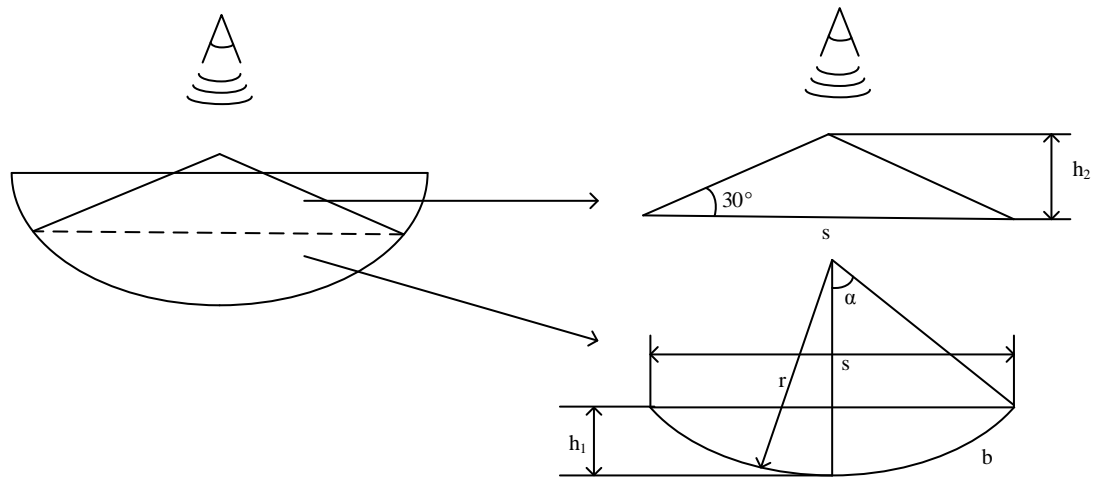


Figure 3.10: The split of the geometries defining the bed. Left is the approximated shape of the conveyor profile and to the right the two geometries separated. The distance b is the arc length of the circle segment.

The PI loops have been changed slightly from the parameters that were initially obtained from the SCADA system, representing those used in the PLC where the control loops are implemented. In Table 3.1 the parameters K_p and T_i are noted for the simulation and those used by the real plant. The standard PI controller in MATLAB Simulink was used in the simulation. The parameters used in the model were slightly adjusted for the model to be able to handle start up sequences without any added logic. The tuning of the parameters was done iteratively by simulating the model and monitoring outputs and control signals.

Table 3.1: The parameters of the PID-loops on section 406 both the ones used in the model and on the actual plant.

Controller	model: K_p	model: T_i	Plant: K_p	Plant: T_i
Silo Feeders	0.2	14	0.2	14
Silo Feeder SP	1.5	300	1.5	300
HPGR bin Feeders	0.2	150	0.2	300
HPGR feed conveyor	0.2	50	0.7	150
HPGR roller speed	0.2	220	0.65	120
HPGR screen feeder 1	-2	40	-2	40
HPGR screen feeder 2	-2	40	-1.8	40

The controllers in the PLC also have specification regarding deadband included in them, typically around 5% of the setpoint. The controllers used in the simulation model did not include those.

Interlocks were only implemented around the HPGR feeding arrangement, blocking the chute from becoming overfull and allowing for catching up if the level in the chute was lost during operation. One major difference between the model and the actual plant is that the advanced controller used to regulate the level in screen bin

has not been implemented. The screen bin is instead controlled to maintain a 50% level with a PI-controller.

3.2.2 MPC development

The first step to develop a new controller is to investigate if there are enough degrees of freedom in the circuit to reach all set-points for the controlled variables. Reaching all set-points is only possible if the number of manipulated variables (MV's) is equal or greater than the number of Controlled variables (CV's). The manipulated and controlled variables are listed in Table 3.2.

Table 3.2: A list of the considered MV's and CV's

CV	MV
BIN001 Level	FE001/2
BIN002 Level	FE003/4
HPGR Chute weight	FE005/6
CV002 Level	CV002 conveyor speed
-	HPGR roller speed

The actuators listed in Table 3.2 are available for us to control. The HPGR chute weight is essential to keep the crusher choke fed. The level on the **CV002** can be controlled by use of feeder **FE003** and **FE004**. The speed of conveyor **CV002** will regulate how quickly material arrives in the crusher chute. The feeders and the conveyor speeds are coupled, and both are required to keep the chute full. If level on the belt needs to be controlled or not can be investigated, however since this is included in the current set up it was kept.

Removing two CV's and two MV's from Table 3.2 the number of MV's is still larger than the number of CV's, hence there is room for an additional control objective. After confirming that there are enough degrees of freedom in the system to maintain all wished set-points, the controller can be developed. An MPC controller consists of a process model of suitable form, in this case when using the solver software FORCES Pro [13], a state space model, additionally a cost function and if needed constraints. The cost function includes the set-points and possible minimization or maximization objectives. The software solves a quadratic program (QP-problem). On the form is shown in Equation 3.14. The solver also allows for adding limits on upper and lower bounds on state variables and inputs, as well as inequalities on states and inputs.

$$\begin{aligned}
 &\text{minimize} && \mathbf{x}_N^T \mathbf{P} \mathbf{x}_N + \sum_{i=0}^{N-1} \mathbf{x}_i^T \mathbf{Q} \mathbf{x}_i + \mathbf{u}_i^T \mathbf{R} \mathbf{u}_i + f_x^T \mathbf{x} + f_u^T \mathbf{u} \\
 &\text{subject to} && \mathbf{x}_0 = \mathbf{x} \\
 &&& \mathbf{x}_{i+1} = \mathbf{A} \mathbf{x}_i + \mathbf{B} \mathbf{u}_i \\
 &&& \underline{\mathbf{x}} \leq \mathbf{x}_i \leq \bar{\mathbf{x}} \\
 &&& \underline{\mathbf{u}} \leq \mathbf{u}_i \leq \bar{\mathbf{u}}
 \end{aligned} \tag{3.14}$$

FORCES Pro is a fast numerical solver for embedded controllers that once generated

have available Simulink blocks to carry out the optimization on-line in the simulation environment. This is an underlying requirement when developing and testing a controller in Simulink coupled to a simulation model, as the one developed in this work.

The original optimization problem was reformulated into deviation variables in order to be able to punish the optimization objective if the controls change quickly. This is done mainly to achieve smoother control signals. The transformation of the problem results in Equations 3.15.

$$\begin{aligned}
& \text{minimize} && \sum_{i=1}^N \frac{1}{2} z_i^T H_i z_i + f^T z_i \\
& \text{subject to} && D_1 z_1 = c_1 \\
& && C_{i-1} z_{i-1} + D_i z_i = c_i \\
& && z_{i,\min} \leq z_i \leq z_{i,\max}
\end{aligned} \tag{3.15}$$

3.2.2.1 The process model

The input to this model is the result of the previous control signal times the control model. This is achieved by supplying c_1 , which is defined in Equation 3.16.

$$c_1 = - \begin{bmatrix} A & B \\ \mathbf{0} & I \end{bmatrix} \begin{bmatrix} x_0 \\ u_0 \end{bmatrix} \tag{3.16}$$

The C_{i-1} matrix includes matrices A and B which now will be used as the model within the controller. The entries in A and B are visualized as dots in a graph in Appendix B. The matrices A and B describes the process which is to be controlled. The matrix C_{i-1} is assembled in Equation 3.18 and D_i in Equation 3.19. The matrix H consists of the weights for how the model should value the different objectives in the optimization and to penalize the use of the controls. The vector z_i consists of the state variables, the values of the control signals and the change in the control signals. The vector is stacked as shown in Equation 3.17 where each of the entries are vectors.

$$z_i = \begin{bmatrix} \Delta \mathbf{u}_i \\ \mathbf{x}_i \\ \mathbf{u}_i \end{bmatrix} \tag{3.17}$$

$$C_{i-1} = \begin{bmatrix} \mathbf{0} & A & B \\ \mathbf{0} & \dots & I \end{bmatrix} \tag{3.18}$$

$$D_i = \begin{bmatrix} B & -I & 0 \\ I & 0 & -I \end{bmatrix} \tag{3.19}$$

The process model used in the controller was developed with the following assumptions:

- Only tracking mass flow in the controller
- All conveyors represent a fixed delay
- Mass split at the screens is constant during one simulation
- The bins are pure integrators with a fixed capacity

The controller uses a prediction and control horizon of 70 steps, where each step is 10 seconds long resulting in predictions 11 minutes and 40 seconds into the future. No further investigation in how short the horizon could be was made while still achieve good results, however, in general, the prediction horizon should be in parity with the settling time of the system. No experiments were concluded to attempt to find this value. The controller on section 405 uses a 13 minutes prediction horizon, and it was therefore concluded that testing the controller with a 70 step prediction would be the first approach. The FORCES controller has an equally long prediction and control horizon by default, and it was decided to keep it that way for this work.

Using the process layout, the length of the conveyors, the estimated capacity of the bins and the current operating point's split ratio for the screens. The process layout with the notation used in the state space is shown in Figure 3.11. Only one version of this controller was tested, and the objective was chosen to include the two bin levels and to maximize the product on the product belt. Only initial tuning of the controller was done to arrive at a stable and appropriate controller behavior.

The state space model is a 67 state model with a sampling time of 10 seconds. The controller has therefore been placed in a triggered subsystem in the simulation model, which runs every 10 seconds, carrying out the optimization. The three optimization variables, u_1 , u_2 and u_3 are supplied to PID-controllers as set-points. According to the MPC scheme, only the first set of control signals is applied to the process. The method of supplying set-points from the advanced controller to the PIDs is a common approach when using advanced controllers [36]. The developed state space model is not observable in its pure form and needs an observer to work properly. In this case, the bins are sampled with level sensors, the weightometers are located on all conveyors except **CV005** and **CV006**. By sampling the weightometers every 10 seconds and using a shifting buffer, since the conveyors move at constant speed the delay is constant and the number of stored readings depend on the number of states used to model the specific conveyor. This approach is fully possible for the real process as well, with the exception of the belts that do not have weightometers installed. The result is full state access, and there is no need for an additional observer for the controller to work properly.

It is assumed that the first by the controller calculated input acts on the process at time $t + 1$, where t is the current time. The initial condition can therefore be stated as the autonomous response from the previous controller calculation and the current states.

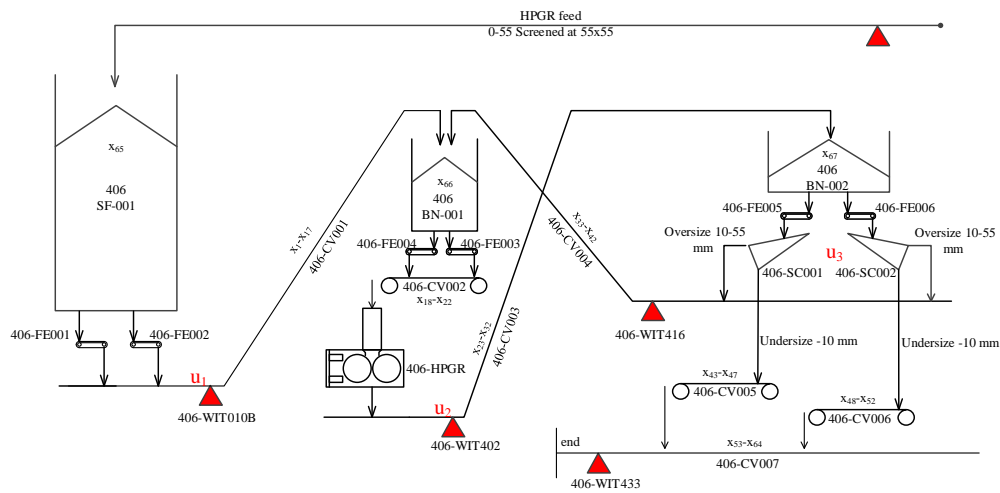


Figure 3.11: The graphical illustration of the state space model used in the MPC controller, The full sized figure is also available in Appendix D

3.3 Model and controller evaluation

The final model and controllers can be used to test many different things, the first wish from Anglo American was to investigate the effect of changing screen decks and how this affects the throughput and inflow for the circuit.

3.3.1 SISO Layered control

Evaluation of the control setup was done by simulating the effect of using different sized screen decks. The test consisted of 5h simulations where the plant started from standing still and was controlled up to its operating point by the PIDs loops only. The performance was evaluated for both a sequence including the startup and a sequence where the start up was removed. The throughput set-point was set to $2400[tph]$, which is what is used today. The inflow was also allowed to increase up to $2000[tph]$.

3.3.2 MPC based supervisory control

The comparison of different screen decks was also done for the MPC controller, simulating four eight hour simulations. The controller was tuned slightly between the simulations. The test included both the startup and the steady state value response. The average startup throughput is based on all eight hours and the steady state based on a six-hour data set.

Apart from the tuning, the split ratio was changed to more appropriate values for the simulation with screen decks of 12 by 12 mm. In the MPC controlled simulations the HPGR crusher was allowed to throttle up to $3100[tph]$, which is the maximum load on the crusher product belt. For the screens to catch up their capacity was also increased to $3100[tph]$.

4

Results

The result of the modeling will first be presented and followed by the results when simulating with the current control setup and the newly developed MPC controller. After that a comparison between the two control setups when changing the apertures of the screens is presented as a simulation case study.

4.1 Model performance

The calibrated model was evaluated based on a measure of normalized mean squared error, as presented in Section 3.1.7. The training data and the validation result is presented in Table 4.1. The label **WIT402p** is the predicted capacity of the HPGR and **WIT402m** is what the feeder is outputting at that instance. This distinction was made since the SCADA data is sampled every 10 seconds and the control of the chute level that makes sure the crusher is choke fed is too fast to be captured in the process data. The actual simulations that resulted in the error estimations in Table 4.1 can be found in Appendix C. The datasets are from the same week, Data set one to three are the 24 hours of November 1st, 2016 and the validation set is from November 2nd from 13:00 to 21:00. Apart from the HPGR model prediction, the conveyor weightometers **WIT416** and **WIT433** have a slightly higher error than **WIT010B** and **WIT402m** this is mainly due to the fact that the screen bin was running empty in some of these simulations, creating a very noisy signal. An example of phenomena in the output flow rate is shown in Figure 4.1 which is from data set 1, also in this figure in the interval 23000 to 27000[s] the product belt is being off loaded and material is placed on the ground instead of in the mill feed silos. This shows up in the data as material missing on the product belt, only because these feeders have been placed before the weight sensor on the product belt. These extra feeders are operated manually, and it's not possible to know when they have been used, apart from the fact that the data looks to be missing material on the product belt. This will, of course, increase the model error and could be removed by disregarding that part of the dataset.

Error estimates for the bin levels were also obtained, however not with the same accuracy as the mass flow. These are presented in Table 4.2. The numbers indicate

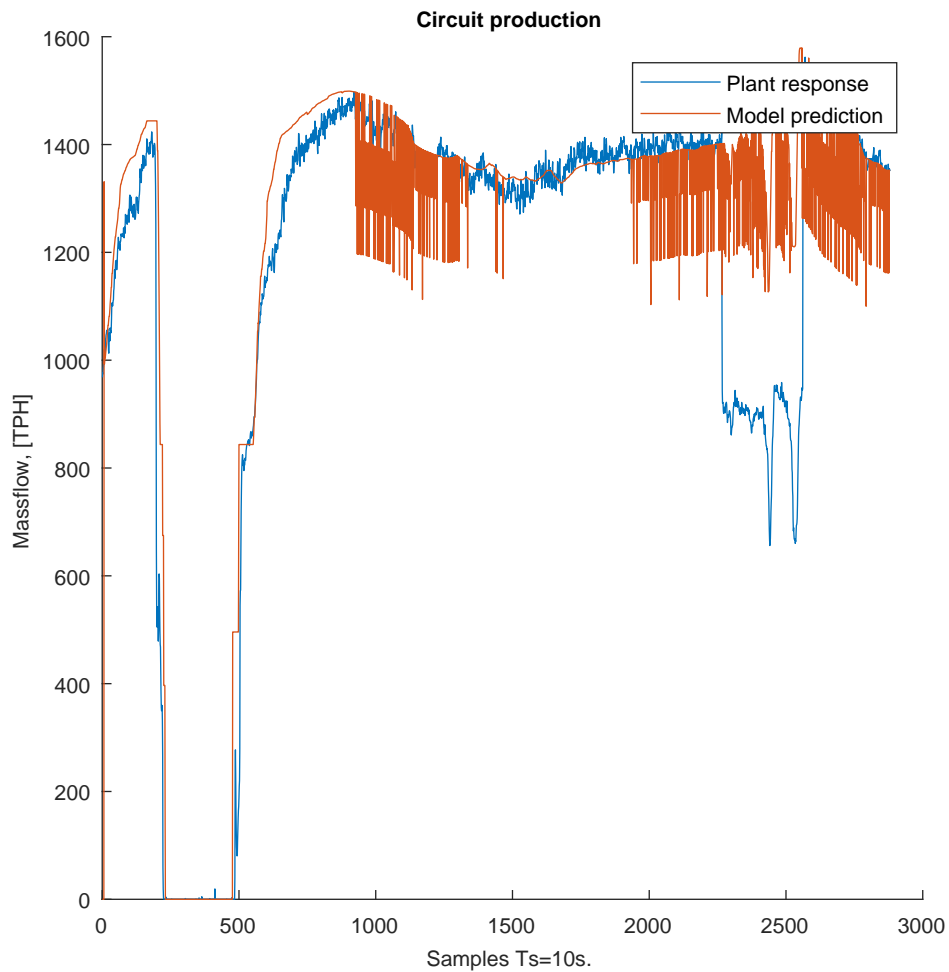


Figure 4.1: The model response for the circuit production with dataset 1, illustrating the result on the output of a empty screen bin during the time intervals when the model prediction is oscillating.

Table 4.1: The NRMSE values of the model compared to the plant data for 4 different data sets, a perfect match between the plant data and the model corresponds to a NRMSE of zero.

	WIT010B	WIT402m	WIT402p	WIT416	WIT433	Average
Data set 1	0.0730	0.0459	0.1404	0.1202	0.1756	0.1110
Data set 2	0.0567	0.0430	0.0489	0.0359	0.0632	0.0495
Data set 3	0.1588	0.0758	0.1650	0.1325	0.1715	0.1407
Validation Set	0.0669	0.0369	0.1159	0.0678	0.0642	0.0703
Average	0.0888	0.0504	0.1175	0.0891	0.1186	total: 0.0929

Table 4.2: The NRMSE values of model correspondence to the plant data for the bins for 4 different data sets

	LIT100	LIT101	LIT405	LIT406	Average
Data set 1	0.6691	0.4675	0.7719	0.7464	0.6637
Data set 2	0.5923	0.3966	0.5291	0.5070	0.5063
Data set 3	0.3295	0.2005	0.6149	0.5918	0.4341
Validation Set	0.4479	0.5142	0.5495	0.4677	0.4948
Average	0.5097	0.3947	0.6164	0.5780	total: 0.5247

that the HPGR bin is slightly better calibrated than the Screen bin. Calibrating an 8 hour integrator is difficult and it has not been the primary goal of this model to exactly describe the behavior of the level sensors. The graphs of the bin level results for the same four datasets can be found in Appendix C.

4.2 Current control layer

The current control setup have been simulated, where the control structure is the same as the actual plant, however a few of the PID control loops parameters have been changed slightly. These are noted in Table 3.1. The simulation results shown in this Section and in Figure 4.2 - 4.6 are for the same 8 hour simulation. The simulation were started from standstill, using no start up sequence. The simulation model ran at the current operating point of the plant. The set-point of the HPGR crusher have been set to 2400 [tph] and the set-points for the bin levels to 55% for the HPGR bin and 50 % for the screen bin.

In Figure 4.2 the output of the circuit is visualized for the entire simulation. The output is oscillating in the beginning of the simulation before it stabilizes to about 1350 [tph]. Some of the oscillations are due to the controller and also partly since the plant is started without any startup sequence.

The HPGR throughput along with the roller speed control signal is for the simulation is shown in Figure 4.3. The results indicate that the parameters used for the controller could be tuned to arrive at a better control performance of the HPGR roller speed controller since the set point for the roller speed is oscillating at the beginning of the simulation. The right side of Figure 4.3 the level in the HPGR bin is plotted and it is oscillating the entire simulation but approaching the steady state level of 55% level in the bin towards the end of the simulation. The only way to control the level in the bin is by regulating the inflow to the circuit, and the actual bin level is affected by both the inflow, the circulating load and the HPGR throughput. The stabilization of the bin level therefore requires the other two affecting mass flows to stabilize before the level can stabilize.

The output of the screen feeders and the screen bin level is visualized for the simulation in Figure 4.4. During the calibration of the simulation model the screen feeders were found to work at different rates, the second feeder was found to feed with a higher rate than the first feeder. This is assumed to be the effect of the material being unevenly placed in the bin. In the simulation model, the material is placed evenly between the two sides of the bin, resulting in feeder two slowing down to still

4. Results

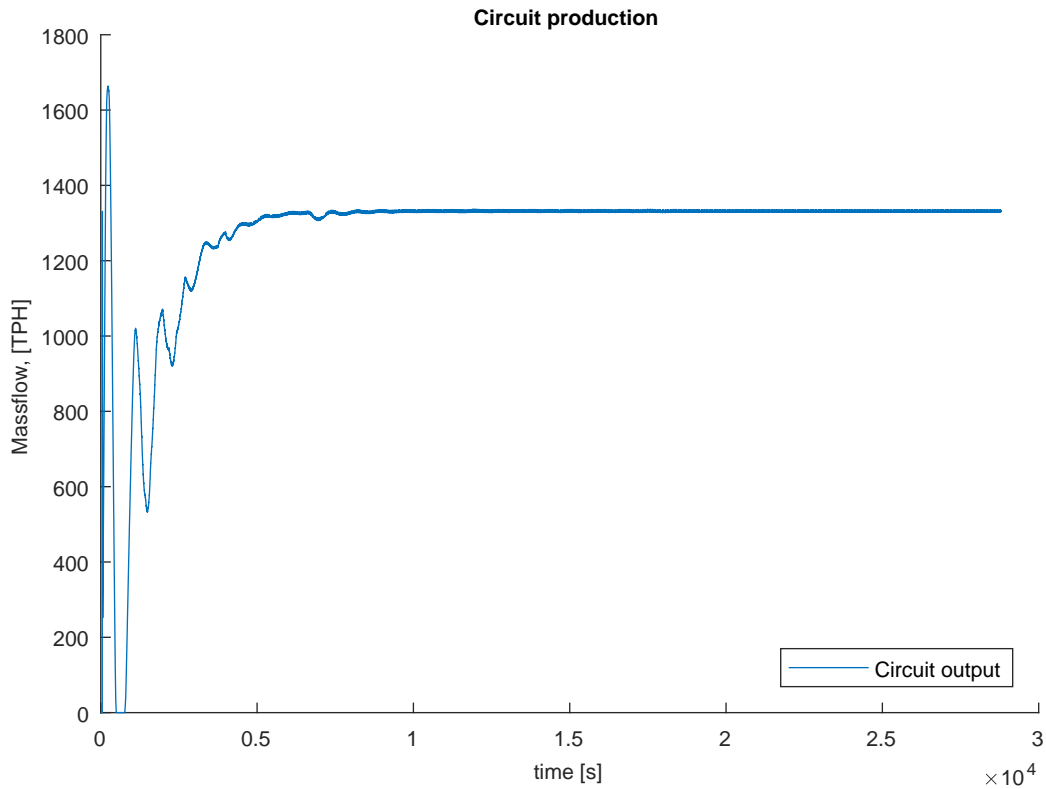


Figure 4.2: The production rate of the circuit over an 8-hour simulation with the current control layer.

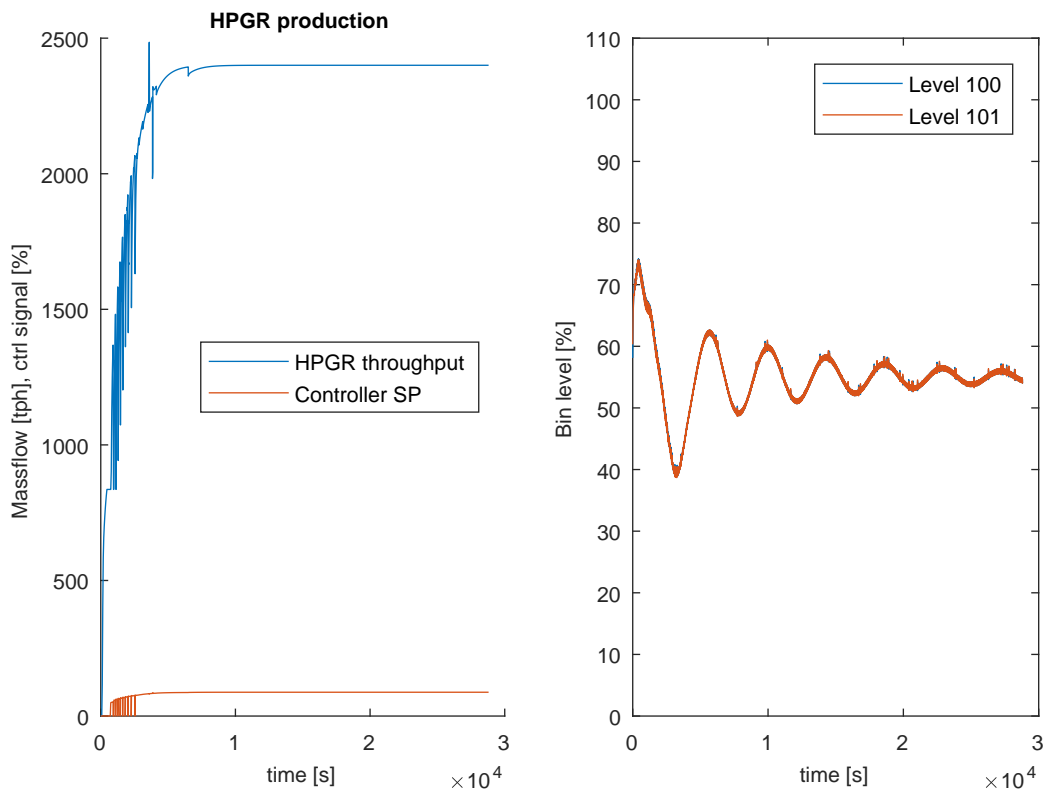


Figure 4.3: (Left) the HPGR throughput and the control signal. (Right) The level in the HPGR bin.

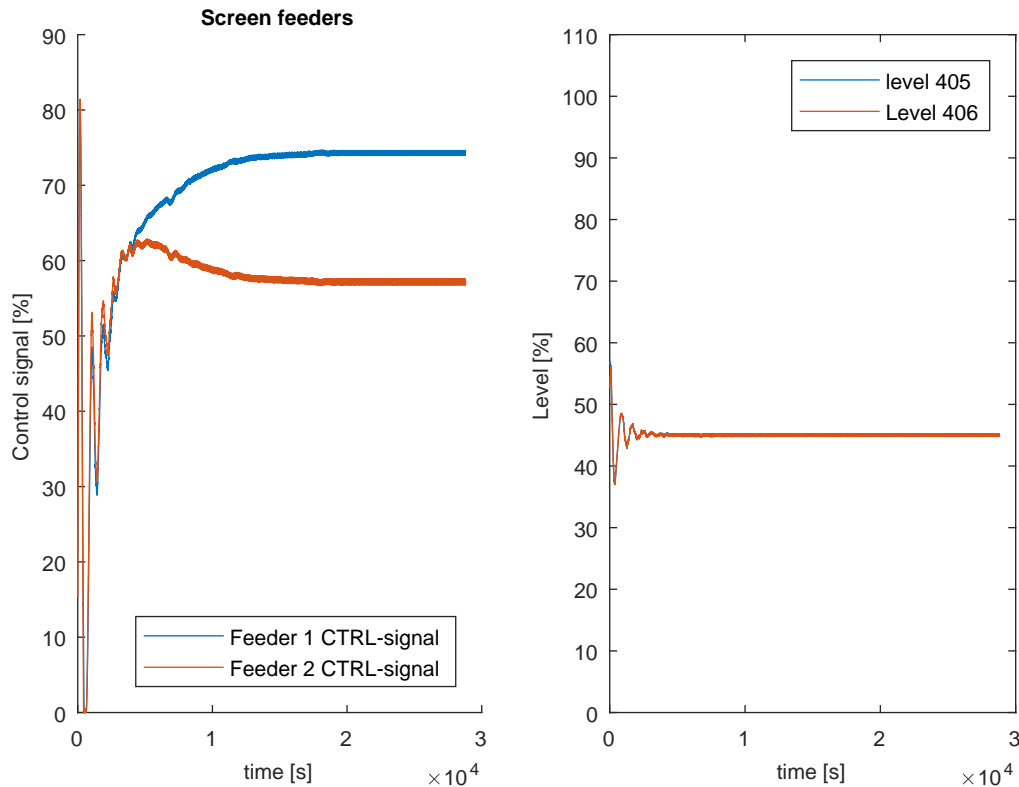


Figure 4.4: (Left) The resulting control signals for the two screen feeders. (Right) The level in the screen bin.

control the level to 50 % for both sides of the bin. In Figure 4.5 the inflow rate and the circulating load are plotted. The circulating load stabilizes after about 2 hours of the simulation, and the inflow tries to regulate the level in the HPGR bin. The settling time of that control loop is very long in addition to the reasoning regarding the level in the HPGR bin. The circuit inflow was saturated between 280 and 1900 [tph].

One important requirement when using the HPGR is that the crusher is choke fed. In Figure 4.6 the weight of the chute for the 8 hours simulation is shown, the interlock function will stop the feeders if the weight increase over 10 tons and change the HPGR speed to 25 % if it goes below 2 tons. During the simulation, the level is oscillating in the beginning and stabilizes to the set-point of 6 [tons] after about 1,5 hours.

The performance of the control layer was not compared to logged control signals from the actual plant for any validation purposes. A comparison of this type would be fruitful in assessing how well the replicated setup corresponds to the actual one. The version of the control system simulated in this work shows that the plant model can be controlled into its steady state level for the given inputs. The response time of some of the controllers is very slow, and no attempt has been made to reduce the response time. However, this could be beneficial for the real plant, being more flexible in the start and stop situations. The actual plant currently has a start-up time of 45 to 60 minutes; the simulated HPGR controller reaches its set-point after

4. Results

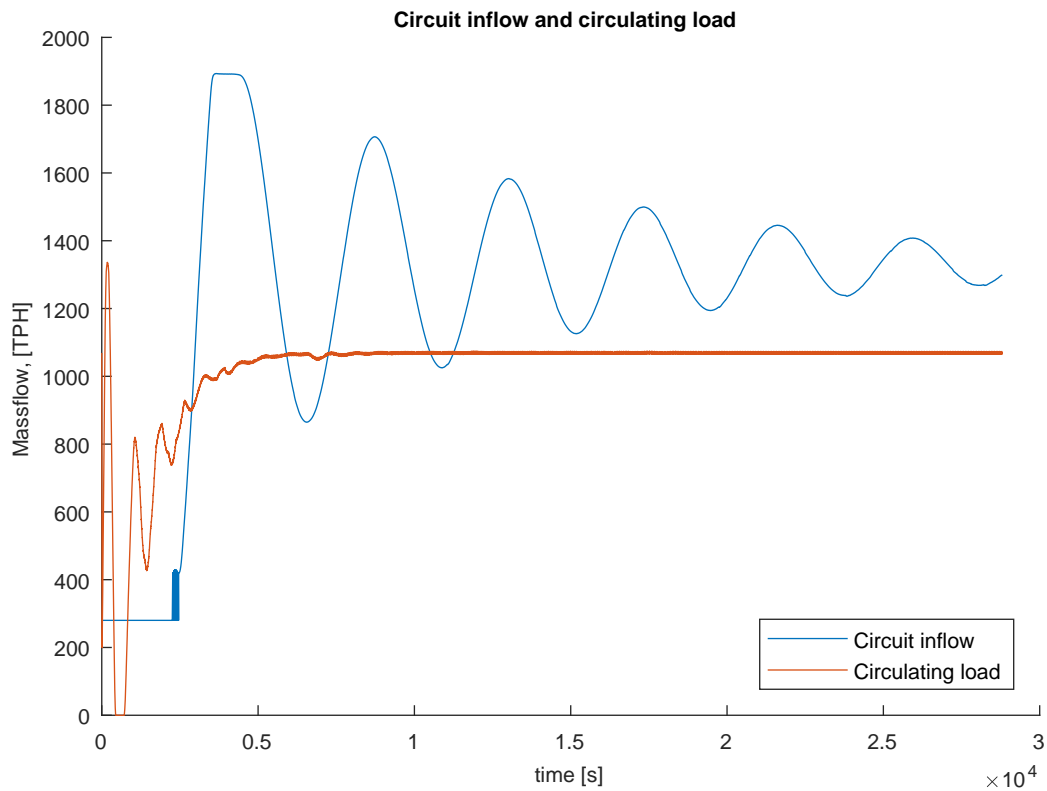


Figure 4.5: Inflow to the circuit and the circulating load for an 8-hour simulation with the current control setup.

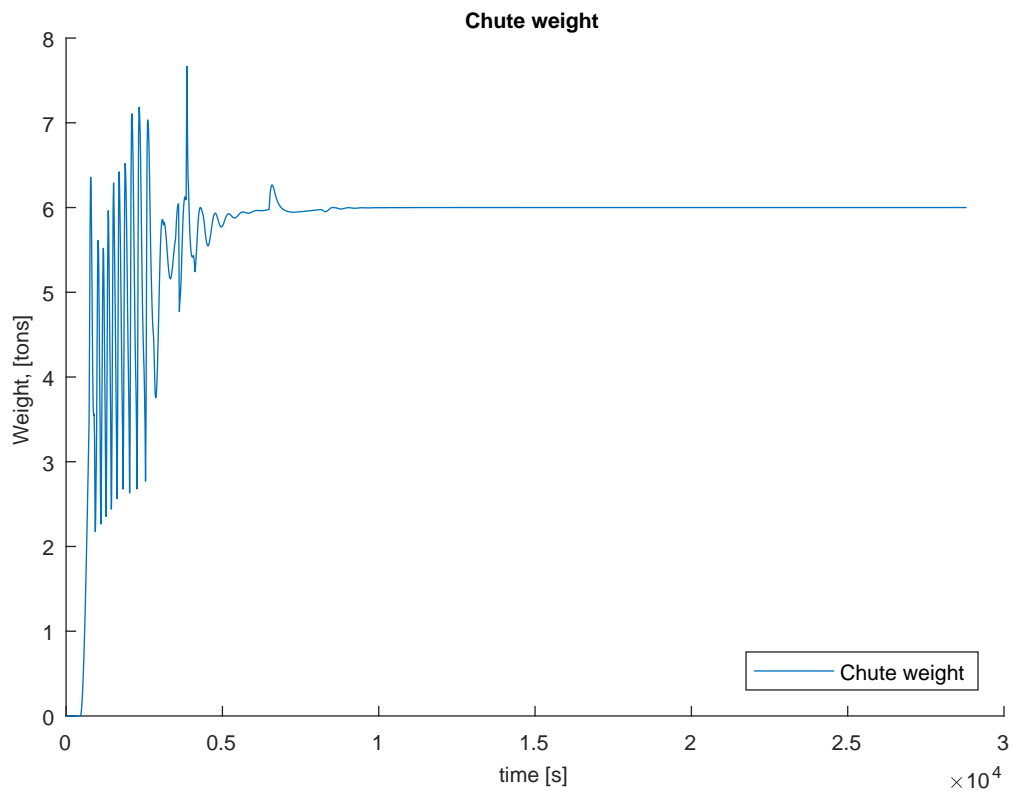


Figure 4.6: The chute weight for an 8-hour simulation.

roughly 1,5 hours. This indicates that the replicated control system is slower than the actual plant.

4.3 MPC controller performance

The MPC controller was used to investigate a potential upside of the production at section 406 at Mogalakwena North by the introduction of a new controller. The plots are the result of a simulation using the current circuit configuration adapted for use with an MPC controller. This includes skipping the coupling between the inflow feeders and the level in the HPGR bin and introducing a new PID controller that controls the screen feeders. For the screen feeders, since there is no available weightometer around them, a model was used to supply the PID controller with a process value.

The HPGR was limited to 3100[tph] as that is currently the maximum load the product conveyor can take. The HPGR bin feeders and the screen bin feeder were also allowed to throttle up to 3100[tph]. The Figure 4.7- 4.11 show the controlled variables, the output and the computation time for the controller for an 8-hour simulation. The simulations were carried out on a Dell Latitude e5430 with an i7-3540M processor and 16 Gb RAM running MATLAB Simulink 2017a [19].

The simulation results show that the MPC controller can control the circuit over a longer period. The here simulated case includes a maximization criterion which pushes the controls to max and risk instability in a real world situation. This should be kept in mind, especially since the prediction horizon's size for the specific circuit have not been thoroughly investigated in this work. Also the since the HPGR and the screen feeder have the same output rate the only way to reduce the level in the screen bin is to cut back on the HPGR when both controls are at maximum.

The rise time when using the MPC to feed set-points is fairly long in this case, additionally since the MPC was in control from the start of the simulation and not to risk instability the control actions were limited. In Figure 4.7 the output is oscillating in the beginning due to the controller supplying inconsistent set points and failing to find optimal solutions to the optimization problem. The output settles to 1725[tph] after little over 2 hours of the simulation.

The bins were started at 50% and 60% filled respectively and the Screen bin reaches its set point first of the bins. This can be seen in Figure 4.9. The start up of the HPGR is slow; this is an effect of the carefulness needed to increase the speed of the HPGR without risking to loose the level in the feed chute to the crusher. This causes the MPC controller to overestimate the amount of material needed to supply the feed bin with, and the level grows up to just under 90 % before the HPGR catches up. This can be resolved by tuning of the controller, especially the slew rate. The rise of the set point and the output of the HPGR are plotted in Figure 4.8

The inflow during the simulation is shown in Figure 4.10 and is the variable that should be used as to make sure the level in the HPGR bin is kept close to its set-point. It is over predicting the rate at the beginning of the simulation, because of the reason mentioned above, after that it settles in and reaches a level at 1700[tph]. The feeder PI-controller that uses the set-point is fast and the difference between

4. Results

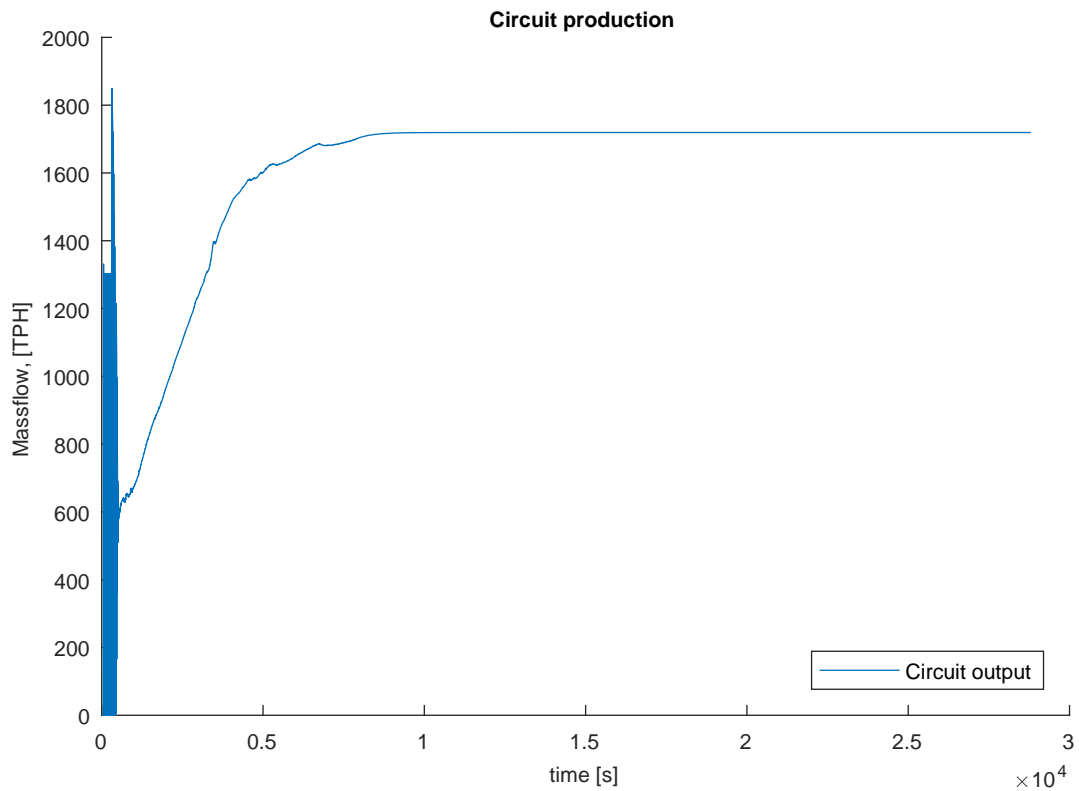


Figure 4.7: The result of the using an MPC to regulate the process, when maximizing output on the product belt **CV007**.

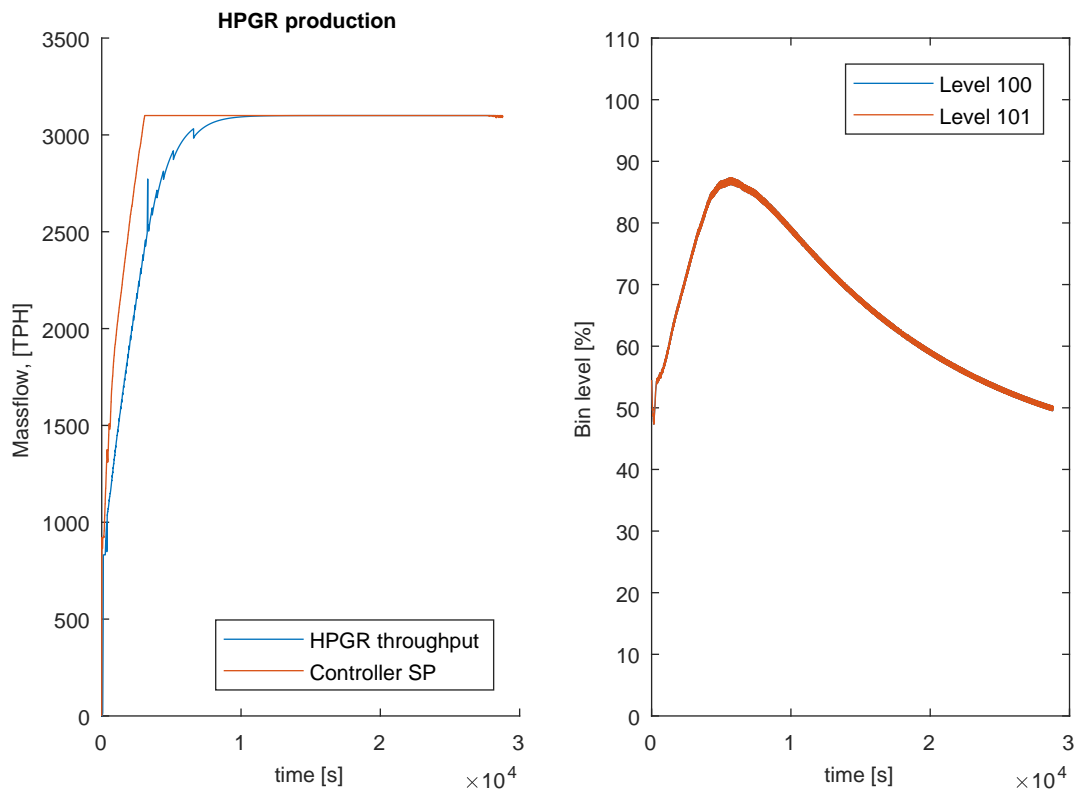


Figure 4.8: (Left) HPGR crusher throughput and (Right) HPGR bin level

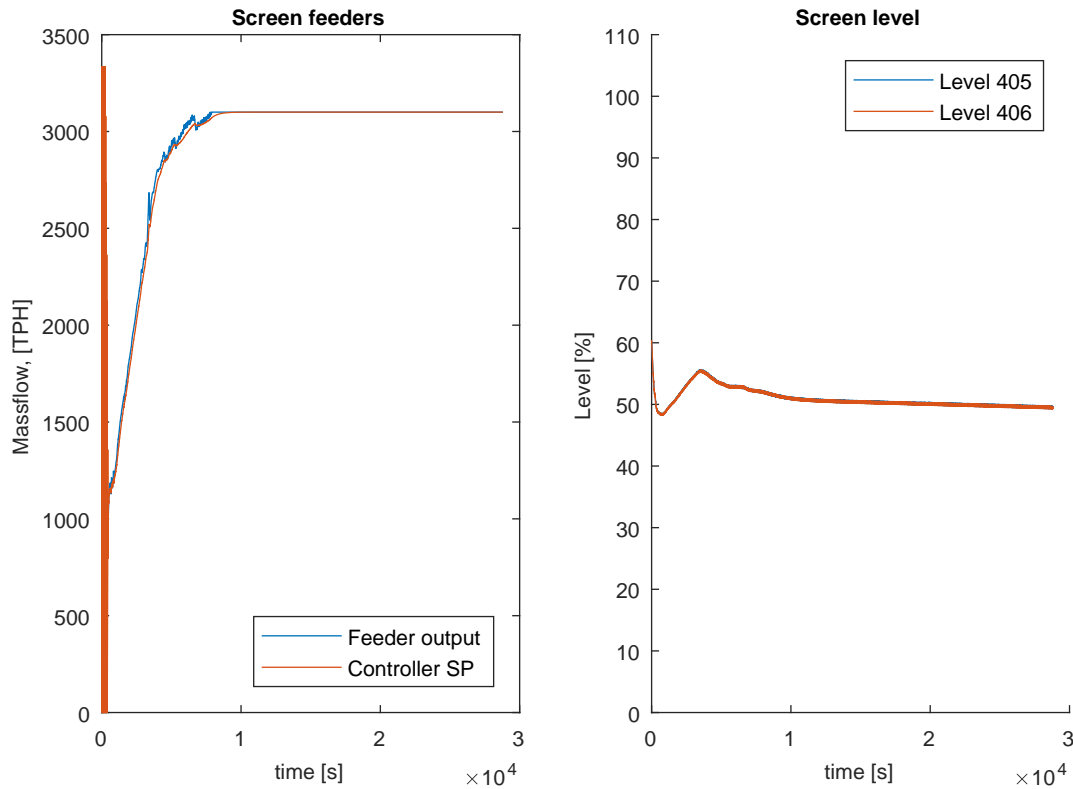


Figure 4.9: (Left) Screen throughput and (Right) Screen bin level

the two signals is hardly visible and is more similar to what the HPGR output and its set-point should do with a better tuned controller. The optimization solver from FORCE Pro solves a QP-problem of 5180 variables on a standard laptop in a time between 1 and 4 seconds. The first part of Figure 4.11, where some iterations took up to 20 seconds, can be eliminated by reducing the maximum number of iterations the solver can do and making sure the observer used was initialized such that the infeasibility is avoided initially. Another approach to reducing this problem is to run a parallel controller during the startup and switch over to the MPC when it has found feasible solutions for a certain period.

4. Results

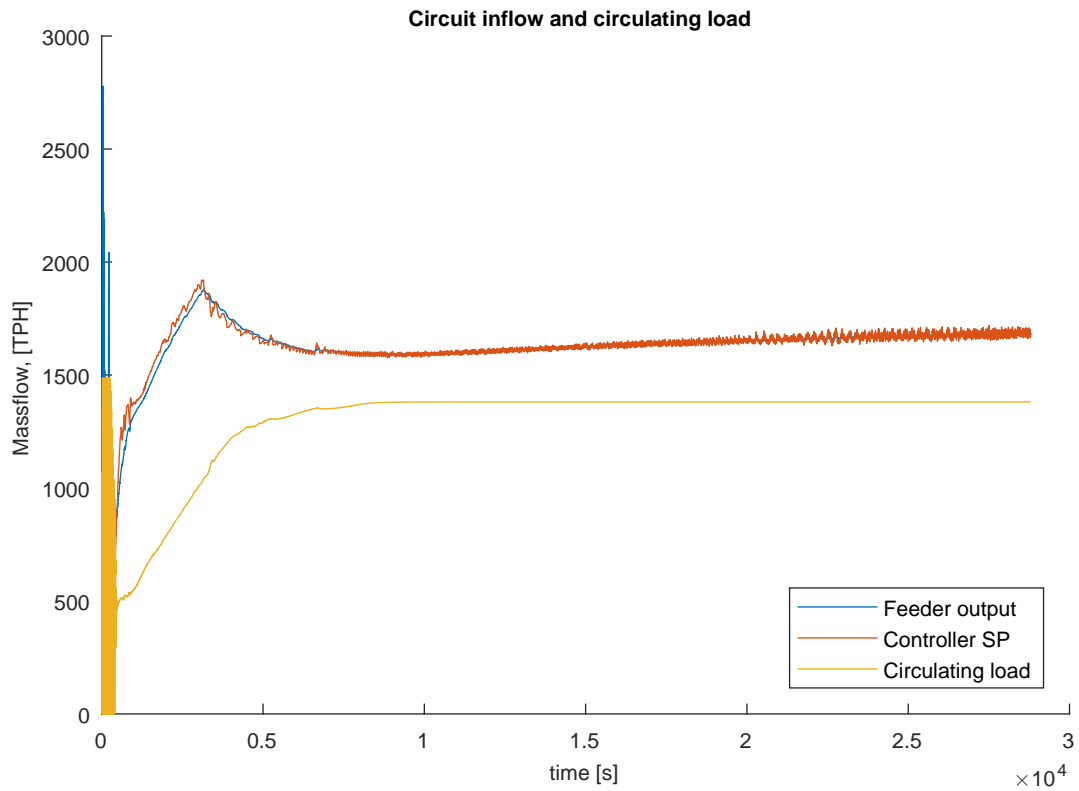


Figure 4.10: The inflow into the circuit from the 406 silo.

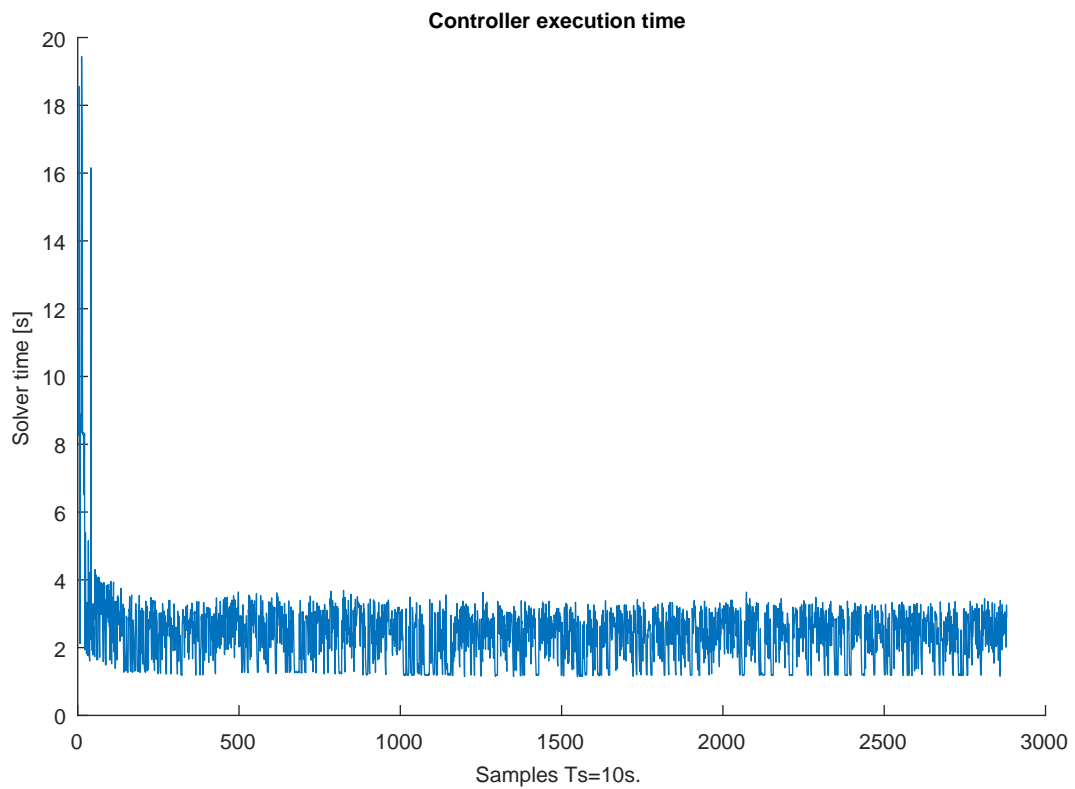


Figure 4.11: Solver time for the controller, the beginning of the simulation the controller may have some problems to find feasible solutions to the control problem.

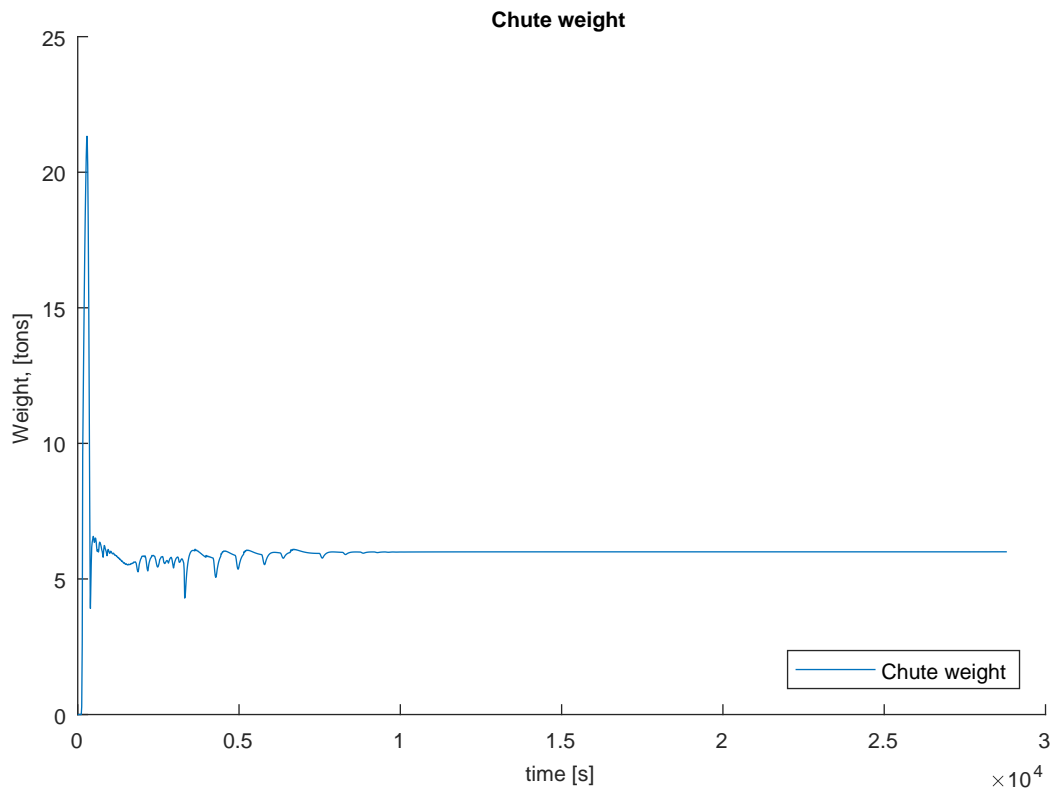


Figure 4.12: The weight of the chute during an 8 hour simulation with the MPC controller.

4.4 Evaluation of circuit changes

During site visits and discussion at the corporate office in Johannesburg, interest was shown in investigating the effect of changing the screen deck apertures; recently the apertures were changed to increase the throughput of the HPGR circuit. The effect on the circuit throughput for different screen apertures have been simulated in this work. The HPGR-screens are today 10 by 10 mm size unworn.

4.4.1 Using the current control setup

When using the current control setup of the plant except the APC based set point selector on the screen bin, Figure 4.13 can be generated. The HPGR throughput set point was set at 2400 [tph] and the rest of the circuit in its original configuration. The screen apertures used for the simulation were 6, 8, 10 and 12 mm. The simulations were started from stand still and therefore the results in Figure 4.13 on the left side are slightly lower since they include the startup sequence. Each simulation ran for 4 hours. Increasing the screen aperture increases the production rate as suspected. The increase from 10 to 12 mm is larger than expected and should be subject to investigation.

4. Results

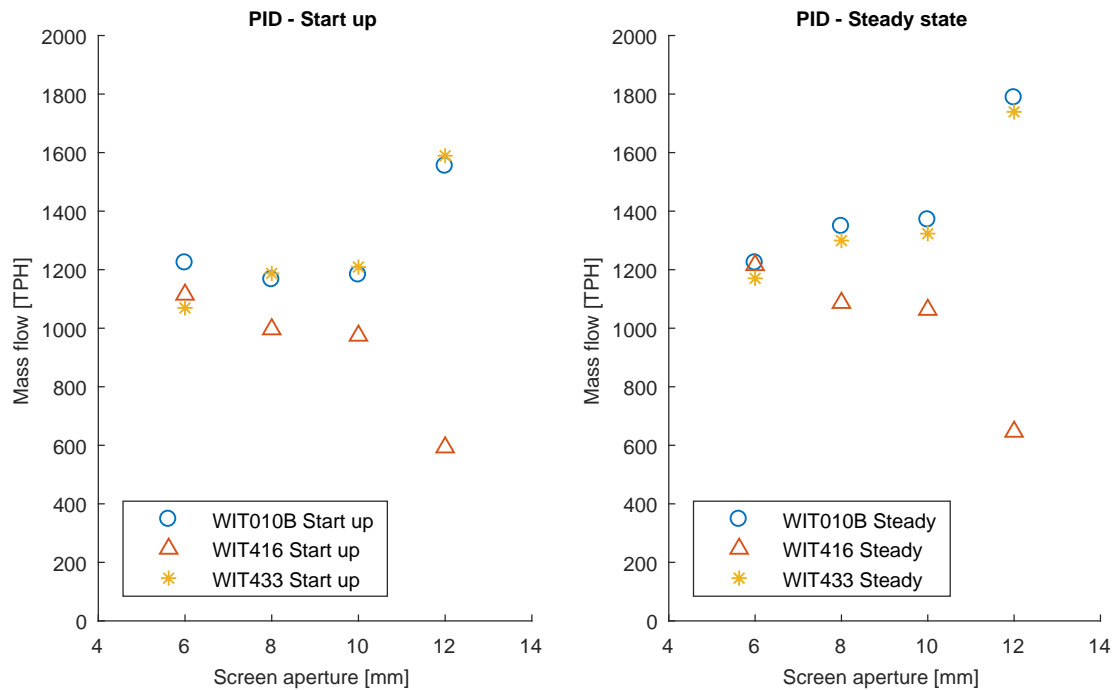


Figure 4.13: Simulation results from 4 different screen apertures for both a startup sequence and a steady state sequence.

4.4.2 Using the MPC

A similar exercise as with the PID set up was done with the developed MPC controller. The results are very similar but here showing a larger throughput. The large step between 10 and 12 [mm] is visible in these simulations as well. The MPC ran for slightly longer than the PID setup, and a simulation lasted 8 hours and the first 2 hours were included in the start up sequence and have been omitted when calculating the steady state values in the right plot of Figure 4.14.

4.4.3 Comparing the two controllers

In Figure 4.15 the two controllers are compared regarding the tonnage placed on the circuit product belt, **CV007**. In general, the MPC controller can output more than the PID controlled circuit. The MPC had more capacity in terms of the crusher and the feeders, however comparing the difference between calculating the set-point once every ten seconds and having an operator overseeing it is preferable to have it supervised by the controller. Being surer the circuit is stable, in essence, allows for selecting a higher throughput as the operating point. The results in Figure ?? shows that there is a potential upside in using a model predictive controller to supervise the set points on circuit 406. The main difference between the current control setup is that level in the HPGR bin have all three components affecting it monitored in the controller and especially the circulating load, which previously acted as a disturbance on the level in the bin.

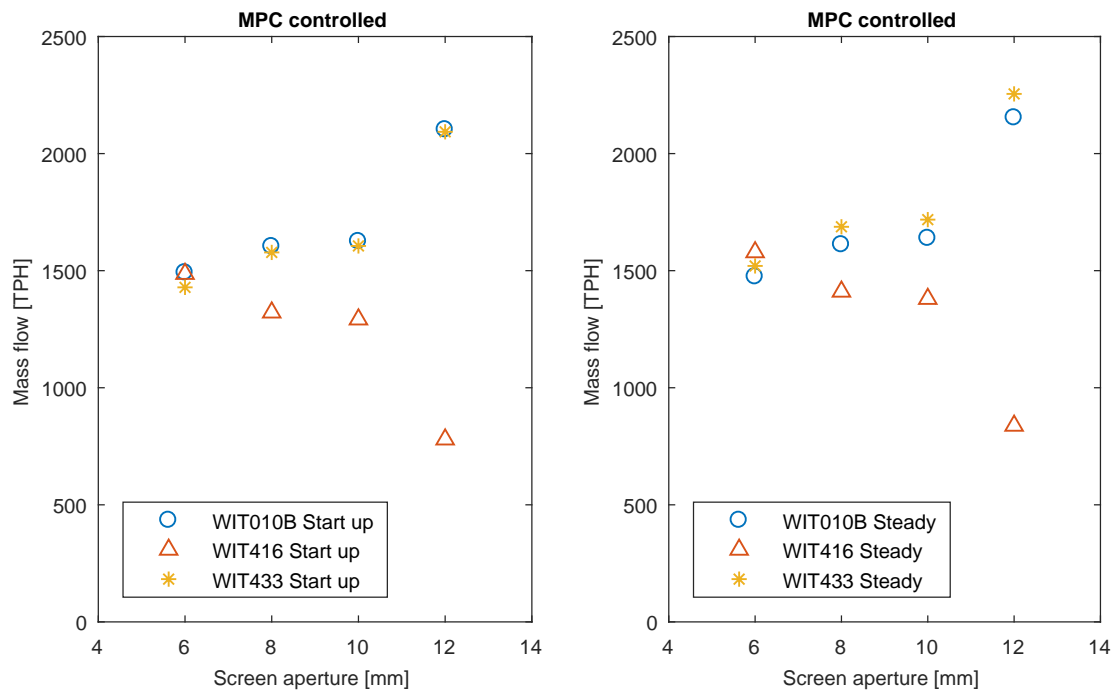


Figure 4.14: Simulation results from 4 different screen apertures for both a startup sequence and a steady state sequence using the newly developed MPC controller.

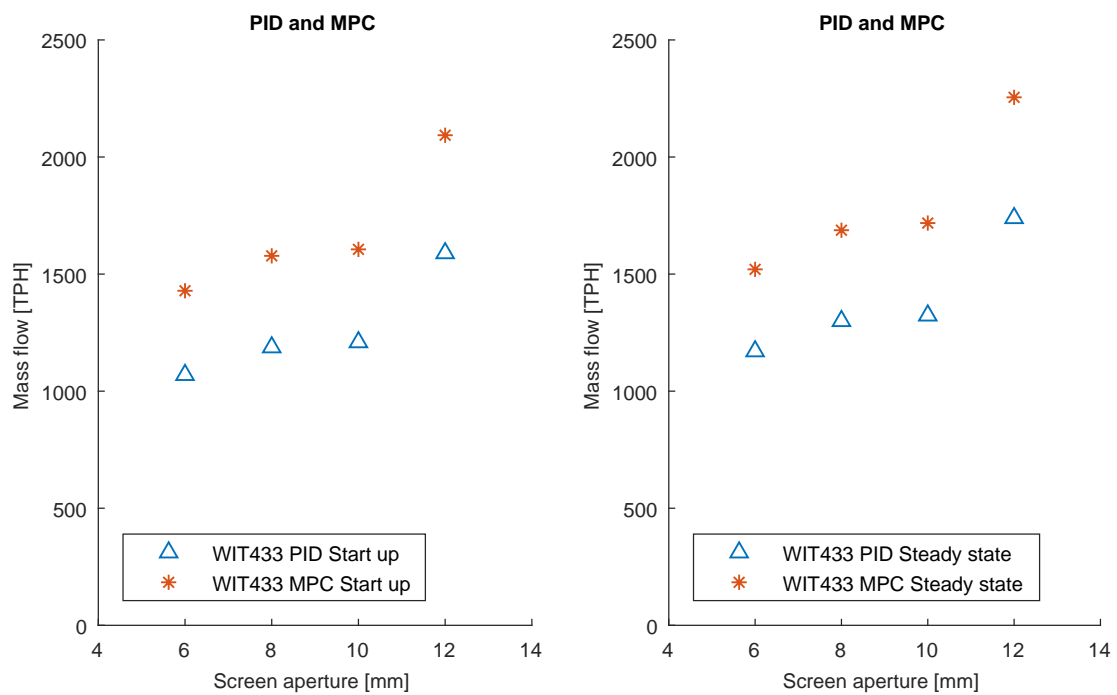


Figure 4.15: Simulation results from 4 different screen apertures for both a startup sequence and a steady state sequence using the current control system.

5

Conclusion

This chapter will present the conclusions from work within the master's thesis and discuss some of the interesting aspects and future areas of work. Also, the research questions will also be answered.

In this work, a time dynamic simulation model of section 406 at Mogalakwena North Concentrator has been developed, tuned, validated. The model has also been used to test the performance of the current control setup and a new more advanced controller. The new controller has been compared to the current circuit configuration. The new controller was after that compared against a baseline operating point of the current circuit and when applying changes to the circuit in the form of changing apertures of the screens. The results show a possible upside in circuit performance if an MPC controller is added to today's control solution. The use of time dynamic models have proven useful and promising for the development of controllers, testing circuit configurations, tuning controllers and evaluating their performance over time.

5.1 The research questions

The following section will answer the research questions stated in section 1.3, the questions are answered one by one and stated before each answer.

5.1.1 Research question 1

- What type of model characteristics are required for time dynamic simulations?

The models used in time dynamic simulations can be of steady state type, however if the equipment or process shows signs of a time evolving response and the previous state of operation matters for the future predictions then time varying components should be included in the model. This holds true especially for the HPGR crusher with its hydraulic system. The models needs to be fast and must avoid iterative calculations that could run into convergence problems as well as instability of the model. Time dynamic simulation models of the type built in this work easily becomes complex systems and therefore it is a big advantage in keeping the models simple and rather introduce an extra tuning factor than an extra integral.

5.1.2 Research question 2

- How can large variation and uncertainties in incoming feed and machine wear be handled in order to increase robustness of control system performance?

The performance of a control system, especially an MPC controller depends on how well it's tuned. There are many methods for tuning regular PID controllers. MPC controller on the other hand requires knowledge about the response of the controller for a change in a certain parameter, there are rules of thumb and how to adjust for example the R and Q matrices for smoother or more aggressive response. The key to successful tuning lies in having good knowledge of both the controller and the process. It will in most cases require some trial and error approach and it is therefore great to have a simulation model to test the controller with.

The effect of variations and can be handled, depending on the variation by estimation of disturbances or on-line estimation of parameters, such as the split ratio at the screen. Using for example an on-line particle size analyzer to signal to the control system if there is more or less material that is going to be circulated in the near future. Handling machine wear can be done in a similar manner, by estimation of critical parameters, logging maintenance. Increased understanding of the process and thereby knowledge of the effect of wear on the process could potentially increase the possibility of choosing the right parameters to tune. One advantage of having access to a calibrated process model is the possibility to test at what stage the controller becomes unable to control the process adequately, this was not tested in this work but is certainly interesting for future work.

5.1.3 Research question 3

- How can model predictive control be applied to a crushing circuit simulation?

A controller for a flow based system can be established by known techniques and be tested in a simulation environment, such as Simulink. With the software FORCES pro this can be achieved without having to write custom made code for the application.

Supervisory controllers are usually executed less frequently than a regular PID controller, and it is therefore needed to be able to handle different sampling times within the system. This can be done in MATLAB using a structure that is triggered. The controller sampling time needs to be an even multiple of the global sampling time. The first stage of applying this type of controller to a crushing circuit is to be able to handle the flow. In future versions, the controller should be able to track and simulate of the bin content and have more adaptive behavior in regards to the quality of the crushing. Using parametric state space models where the coefficients can be changed online means that there is an opportunity to adapt the behavior of the controller if for example the output product size is decreasing or increasing because of changes in the ore.

5.2 Discussion

The primary task of calibrating the dynamic model to correspond well to the process data was a very time intensive task and the framework used for the calibration process was presented in Chapter 3. For future modeling exercises including process calibration, this list will be utilized and along with new ideas of how to complete this process more time efficient. It is likely that the need for these kinds of models will be in high demand in the future and a clear framework and set of reference points would be very helpful.

The model calibration has been done on a data set of 36 hours, and one set of particle size data. The dynamic calibration is believed to be up to standards. The prediction of particles size has been calibrated on one data set which is a risk in terms of only checking circuit correspondence at one point. This should be included in future work to address this issue and obtain data from the circuit under different operating conditions to strengthen the calibration result.

Model predictive control is a control method that has swarmed process industry since the beginning of the 1970s, and there is no incitement that it should not continue to grow, the application areas within minerals processing are endless and the actual use of more effective and optimal systems is beneficial for both the environment, companies and the workers in the long run. Platforms for development and testing of new controllers without impacting the real process will allow for a better chance of deploying a successful new strategy. In terms of developing control schemes and completing initial tuning of controllers, the use of the time dynamic model is great. The non modeled advanced controller to select the set point for the screen bin feeders may not be needed when using an MPC, the target value for the bin level can be set low and the potential of over filling the bin avoided. Over filling can happen in the simulation without consequence, however, on the real plant, the control engineer who is responsible will have to decide on how much redundancy to consider in the system.

The MPC had problems finding optimal solutions at the beginning of the simulation; this is thought to be due to the observer setup. The observer needs to run for many iterations before it is fully initialized. By only starting the observer and letting the circuit be brought up to an idling operating point before letting the MPC start to supply set points should solve the feasibility problem. In an actual real implementation of an advanced controller, a security layer is used to handle these kinds of problems. This layer will also act as a back up if the MPC is unable to find a solution within the time constraint, in this case, 10 seconds.

During the commissioning of the Mogalakwena North Concentrator the basic control layer was initially designed, and in the case of the HPGR circuit, the control loops around the chute feeding arrangement have been updated once. Tuning of the current control set up could potentially increase the benefit of the circuit and improve its performance. These controllers work well in their current configuration. However a speed up of for example the start up sequence could probably be achieved. This would lower the response time during start-up, and the response of a roller speed

set-point change improved in a way that could potentially benefit the circuit.

The results from comparing different screen decks look promising, the potential benefit in the downstream milling circuit from a decrease in particle size should be investigated. The results for screen deck 6, 8 and 10 mm looks fairly good, the 12mm seems to be a very large step in throughput, and this could potentially be an effect of only using one data set for calibrations of the PSD prediction. Another possible explanation might be that the fresh feed has been too sharp causing the crusher product to become bimodal. This should also be investigated to be sure that the results used for potential future decision making are as accurate as possible.

5.3 Future work

This work has spanned many areas, and there are therefore also many extensions and ideas to work with in the future. They are described in this section in a similar structure, split up into modeling and control.

The method used to predict the particle size in the current model should be updated and compared to other methods used in the research community, and it should be investigated if there is a way to adapt the particle size prediction test and methodology by Evertsson [15] to describe the HPGR as accurate as the cone crusher.

The hydraulic system of the HPGR is an interesting component that should be subject to future modeling and include a pressure model to feedback into the model as a pressure component. The Mogalakwena North HPGR has an active dampening system. Modeling and understanding the hydraulic system may eventually lead to an opportunity to integrate the particle size model to operate the machines hydraulic system to achieve better comminution and ultimately increase the machine utilization.

An advanced controller should contain state of the art models for the application and support the possibility to update the model depending on the movement of the process, the tool used for the controller development allows for the parameters of the model to be updated for each stage of the optimization and each prediction stage. A controller that uses the model to linearize the process for each time instance. Also possibly using the future predictions of the controller to linearize around the predicted operating point. Such an approach will create a very adaptive control scheme that will be, given a calibrated model, very responsive to changes in the process. Additional work should be pointed towards concluding research to include particle size, in other words, product quality into the control system and explore the opportunities that arise by being able to control and keep track of process quality in greater detail.

The relationship between a successful controller and the model calibration is an interesting relationship. A correct understanding of this relationship could potentially save time and the effort spent on doing model calibration set in parity with the results expected from the controller and controller tuning.

Bibliography

- [1] Mine profile: Mogalakwena. <http://www.angloamerican.com/media/our-stories/mine-profile-mogalakwena>. Accessed: 2017-05-14.
- [2] Gauti Asbjörnsson. *Crushing Plant Dynamics*. Chalmers University of Technology, 2015.
- [3] Gauti Asbjörnsson, Erik Hulthén, and Carl Magnus Evertsson. Modelling dynamic behaviour of storage bins for material handling in dynamic simulations. In *XXVI International Mineral Processing Congress (IMPC 2012: Innovative Processing for Sustainable Growth; New Delhi; India; 24 September 2012 through 28 September 2012)*, pages 258–267, 2012.
- [4] Gauti Asbjörnsson, Erik Hulthén, and Carl Magnus Evertsson. An on-line training simulator built on dynamic simulations of crushing plants. *IFAC Proceedings Volumes*, 46(16):218–223, 2013.
- [5] LG Austin, DR Van Orden, and JW Perez. A preliminary analysis of smooth roll crushers. *International Journal of Mineral Processing*, 6(4):321–336, 1980.
- [6] Gabriel KP Barrios and Luís Marcelo Tavares. A preliminary model of high pressure roll grinding using the discrete element method and multi-body dynamics coupling. *International Journal of Mineral Processing*, 156:32–42, 2016.
- [7] GKP Barrios and LM Tavares. Simulation of a laboratory scale hpgr using dem.
- [8] H Benzer, L Ergun, AJ Lynch, M Oner, A Gunlu, IB Celik, and N Aydogan. Modelling cement grinding circuits. *Minerals engineering*, 14(11):1469–1482, 2001.
- [9] Karl Björk. Formler och tabeller för mekanisk konstruktion. *Karl Björks förlag HB, Spånga*, 2003.
- [10] NA Chapman, NJ Shackleton, V Malysiak, and CT O’Connor. The effect of using different comminution procedures on the flotation of platinum-group minerals. *Minerals Engineering*, 24(8):731–736, 2011.
- [11] Charles R Cutler and Brian L Ramaker. Dynamic matrix control?? a computer control algorithm. In *Joint automatic control conference*, number 17, page 72, 1980.
- [12] Michael John Daniel and Stephen Morrell. Hpgr model verification and scale-up. *Minerals Engineering*, 17(11):1149–1161, 2004.
- [13] Alexander Domahidi and Juan Jerez. FORCES Professional. embotech GmbH (<http://embotech.com/FORCES-Pro>), July 2014.
- [14] Hakan Dundar, Hakan Benzer, and Namik Aydogan. Application of population balance model to hpgr crushing. *Minerals Engineering*, 50:114–120, 2013.

- [15] Carl Magnus Evertsson. *Cone Crusher Performance*. Doktorsavhandlingar vid Chalmers tekniska högskola. Ny serie, no: 1551. Institutionen för maskin- och fordonskonstruktion, Chalmers tekniska högskola,, 2000.
- [16] DA Holwell and Iain McDonald. Distribution of platinum-group elements in the platreef at overysel, northern bushveld complex: a combined pgm and la-icp-ms study. *Contributions to Mineralogy and Petrology*, 154(2):171–190, 2007.
- [17] Marcus Johansson, Magnus Bengtsson, Magnus Evertsson, and Erik Hulthén. A fundamental model of an industrial-scale jaw crusher. *Minerals Engineering*, 105:69–78, 2017.
- [18] Yi Liu and Steven Spencer. Dynamic simulation of grinding circuits. *Minerals Engineering*, 17(11):1189–1198, 2004.
- [19] MATLAB. *version 9.2.0 (R2017a)*. The MathWorks Inc., Natick, Massachusetts, 2016.
- [20] RE McIvor. High pressure grinding rolls—a review. *Comminution Practices. SME Inc., Littleton, CO*, pages 95–97, 1997.
- [21] Manfred Morari and Jay H Lee. Model predictive control: past, present and future. *Computers & Chemical Engineering*, 23(4):667–682, 1999.
- [22] Chris Morley. Hpgr-faq. *Journal of the Southern African Institute of Mining and Metallurgy*, 110(3):107–115, 2010.
- [23] S Morrell, W Lim, F Shi, and L Tondo. Modelling of the hpgr crusher. *Comminution Practices*, pages 117–126, 1997.
- [24] C Ntsele and G Sauermann. The hpgr technology—the hearth and future of the diamond liberation process. *Publication of the south African Institute of Mining and Metallurgy. Diamonds—source to use*, 2007.
- [25] MS Powell, MM Hilden, Carl Magnus Evertsson, Gauti Asbjörnsson, AH Benzer, AN Mainza, LM Tavares, B Davis, N Plint, and C Rule. Optimisation opportunities for hpgr circuits. In *11th AusIMM Mill Operators’ Conference*, 2012.
- [26] Johannes Quist. *DEM Modelling and Simulation of Cone Crushers and High Pressure Grinding Rolls*. Doktorsavhandlingar vid Chalmers tekniska högskola. Ny serie, no: 4225. Institutionen för produkt- och produktionsutveckling, Produktutveckling, Chalmers tekniska högskola,, 2017.
- [27] R. J. Fouchee R. P. Brown, C. W. Steyn. Improving crusher performance by comparing various control strategies using a validated simulation. In *proceedings for the MEI 10th International Comminution Symposium (Comminution ’16)*, 10, 2016.
- [28] Raj K Rajamani and John A Herbst. Optimal control of a ball mill grinding circuit—i. grinding circuit modeling and dynamic simulation. *Chemical Engineering Science*, 46(3):861–870, 1991.
- [29] CM Rule, DM Minnaar, and GM Sauermann. Hpgr-revolution in platinum? *Journal of the Southern African Institute of Mining and Metallurgy*, 109(1):23–30, 2009.
- [30] JL Salazar, L Magne, G Acuna, and F Cubillos. Dynamic modelling and simulation of semi-autogenous mills. *Minerals Engineering*, 22(1):70–77, 2009.
- [31] Daniel Sbárbaro and René Del Villar. *Advanced control and supervision of mineral processing plants*. Springer Science & Business Media, 2010.

- [32] K Schönert. Aspects of the physics of breakage relevant to comminution. In *Fourth Tewksbury Symposium, University of Melbourne*, volume 3, pages 3–30, 1979.
- [33] Klaus Schönert. A first survey of grinding with high-compression roller mills. *International Journal of Mineral Processing*, 22(1-4):401–412, 1988.
- [34] Monica Soldinger Stafhammar. *Screening of crushed rock material*. Chalmers University of Technology, 2002.
- [35] African Minerals Standards. Certificate of Analysis, Platinum (PGM) Platreef Ore Bushveld Complex, South Africa. Technical report, 10 2015.
- [36] Piotr Tatjewski. *Advanced control of industrial processes: structures and algorithms*. Springer Science & Business Media, 2007.
- [37] Barry A Wills and Tim Napier-Munn. *Wills' mineral processing technology: an introduction to the practical aspects of ore treatment and mineral recovery*. Butterworth-Heinemann, 2015.

A

Pressure response experiments

A.1 Presentation of the pressure response results for the Mogalakwena ore.

The pressure response experiments consisted of six test, T1 to T6 where two different top sizes were compressed. For each top size, the width was varied in three steps, a mono size and a steep and a wide distribution. The distributions are shown in Figure A.2. Each distribution was prepared by hand by mixing different amounts of the sieve size classes to obtain the size distributions. The sample was mixed, and the placed in the piston and die. The piston and die have a diameter of 100mm, and the target bed height was 68 mm. Each sample was compressed to 150[MPa], and the response was recorded. Table A.1 shows the parameters calculated from the fitting to the exponential function along with data regarding particle size and width of the distributions for each test. The resulting experiment output data and the models are graphed in Figure A.1

Table A.1: Calibration of the force response model from the material

	a	b	c	d	x_{50}	σ_n
T1	1,845	6,4230	0,0004	23,828	39,100	0
T2	9,930e-06	34,1187	1,8321	8,1587	28,00	0,295
T3	1,2767	10,6092	0,00087	28,8752	17,700	0,6625
T4	1,7058	6,5781	0,0003869	25,2013	26,800	0
T5	0,000510	26,73268	1,4148	8,29135	20,90	0,4444
T6	0,00014481	34,2038	1,4792	11,1912	14,300	0,5594

A. Pressure response experiments

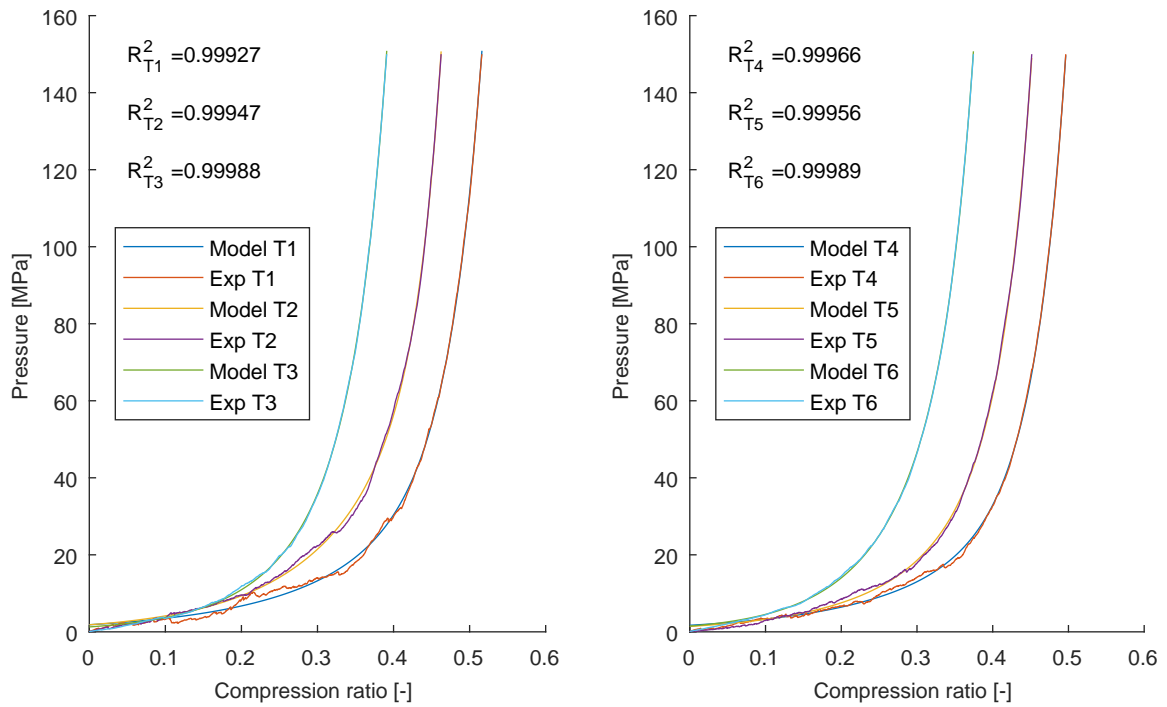


Figure A.1: Resulting pressure responses for all size distributions tested.

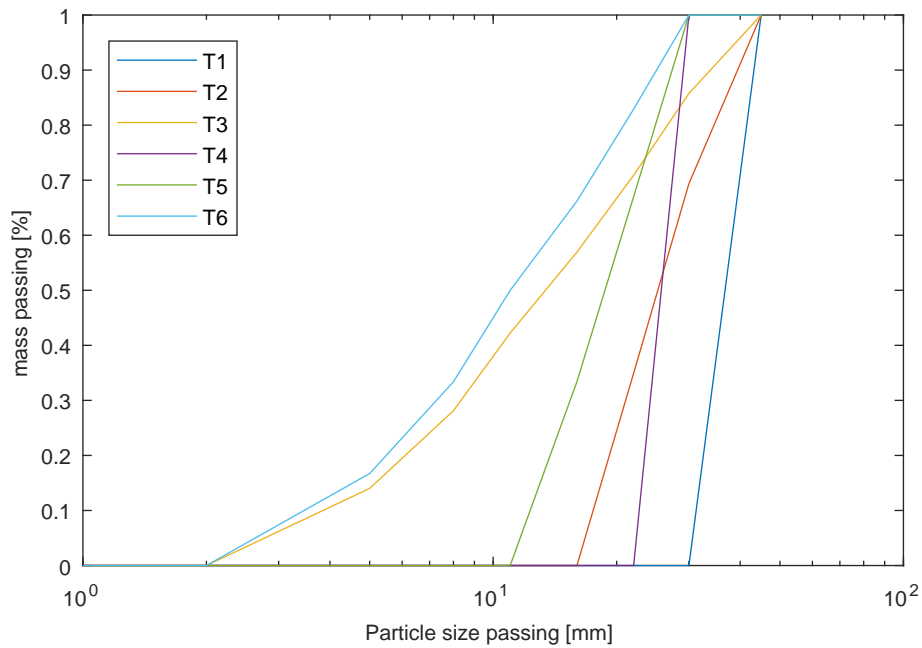


Figure A.2: Particle size distributions used for the compression tests.

B

MPC setup

B.1 Control model

In Figure B.1 are the matrix entries of the controller model of the process pictured. It is the combined result of stacking A and B .

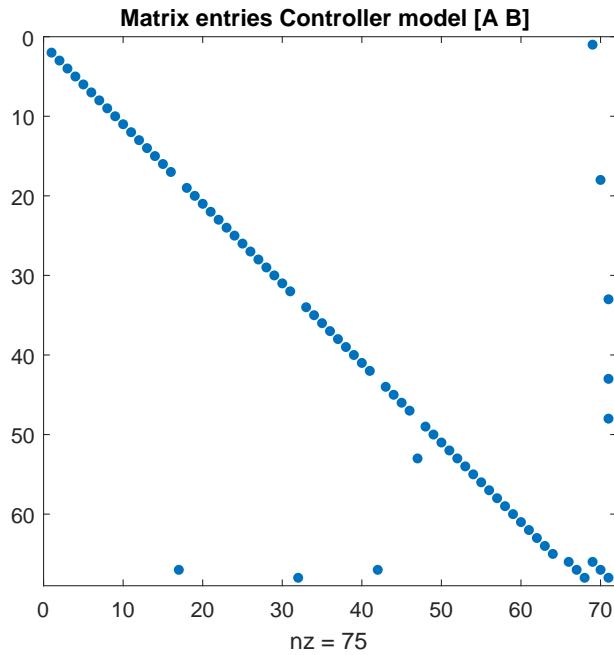


Figure B.1: The A and B matrices where the non zero entries are visualized with a blue dot.

B.2 Control objective and tuning

The control objective used is formulated in Equation B.1

$$\text{minimize}(x_{66} - 100)^2 + (x_{66} - 100)^2 - x_{64} \quad (\text{B.1})$$

The controller constrains are summerized in Equation B.2. All units are in [tons],

[tph] or [tph/10 s].

$$\begin{aligned}
 x_{1-64,min} &= 0 \leq x_{1-64} \leq 5000 = x_{1-64,max} [tph] \\
 x_{65-67,min} &= 0 \leq x_{65-7} \leq 200 = x_{65-67,max} [tons] \\
 u_{1,min} &= 280 \leq u_1 \leq 2780 = u_{1,max} [tph] \\
 u_{2,min} &= 920 \leq u_2 \leq 3100 = u_{2,max} [tph] \\
 u_{3,min} &= 0 \leq u_3 \leq 3100 = u_{3,max} [tph] \\
 \Delta u_{1,min} &= -30 \leq \Delta u_1 \leq 30 = \Delta u_{1,max} [tph/10s] \\
 \Delta u_{2,min} &= -15 \leq \Delta u_2 \leq 15 = \Delta u_{2,max} [tph/10s] \\
 \Delta u_{3,min} &= -30 \leq \Delta u_3 \leq 30 = \Delta u_{3,max} [tph/10s]
 \end{aligned} \tag{B.2}$$

The controller tuning was shifted slightly depending on the simulation case. The original philosophy was to penalize change in control action and make the inflow set point affordable and the HPGR and the screen bin more expensive to change. The weighting on keeping the bin set-points was kept to one. No penalization on high control signals was implemented since in a maximization problem we would like as high control signals as possible without violating the constraints.

The matrix H in the control objective in Equation 3.15 consists of the entries; R and Q .

$$H = \begin{bmatrix} R & \mathbf{0} & \mathbf{0} \\ \mathbf{0} & Q & \mathbf{0} \\ \mathbf{0} & \mathbf{0} & \mathbf{0} \end{bmatrix} \tag{B.3}$$

R penalizing the change in the control signals and Q the deviation of the states from the set-points. In this case, Q only have non-zero entries at position (67, 67) and (68, 68) which is the screen and HPGR bin level states.

The first entry in R was 100 times smaller than the two remaining diagonal entries, implying that the change of the inflow is less penalizing than that of the screen feeders and the HPGR set-point.

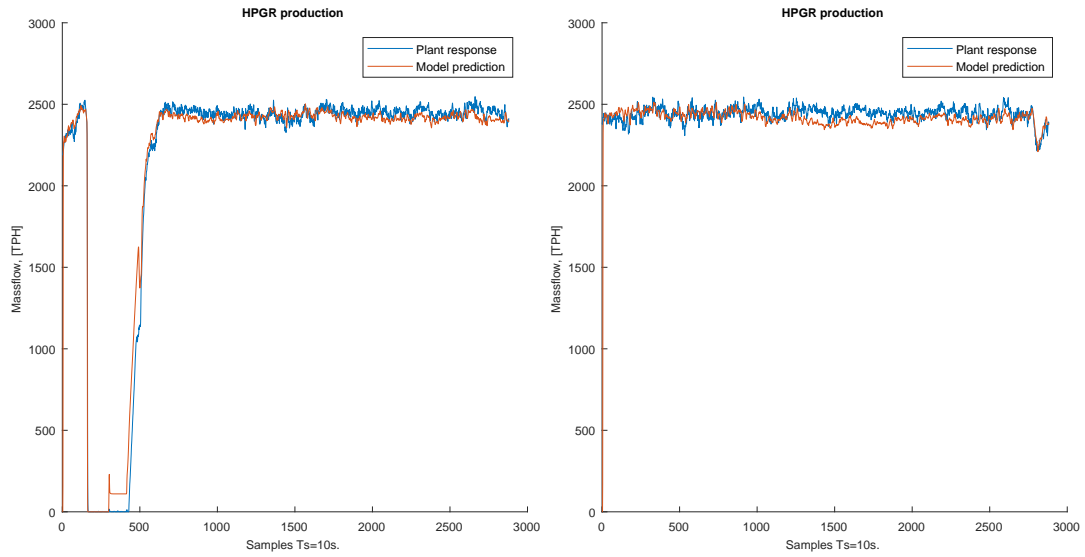
The linear term f in the objective, which is a vector and have negative entries on position (66,1), (67,1) and (64,1). For the set points to be correct, the two set-points for the bins are multiplied by 2.

C

Model calibration Figures

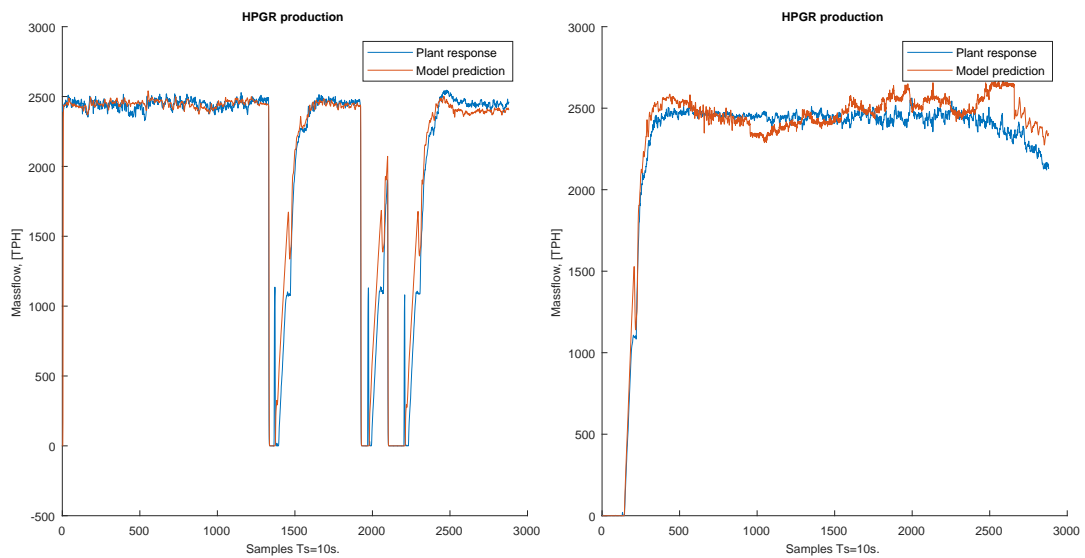
C.1 Training dataset and validation set

C. Model calibration Figures



(a) dataset 1

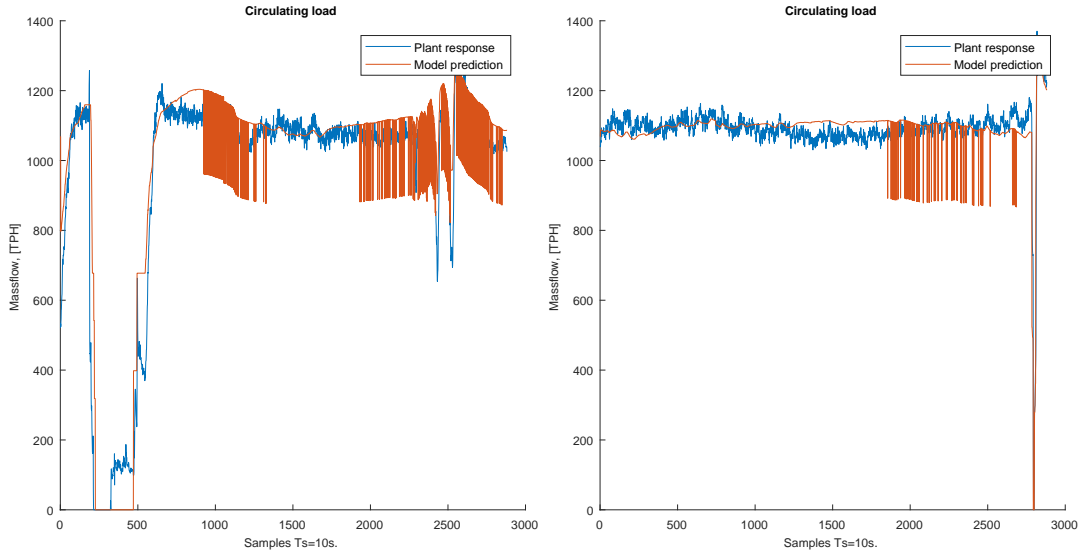
(b) dataset 2



(c) dataset 3

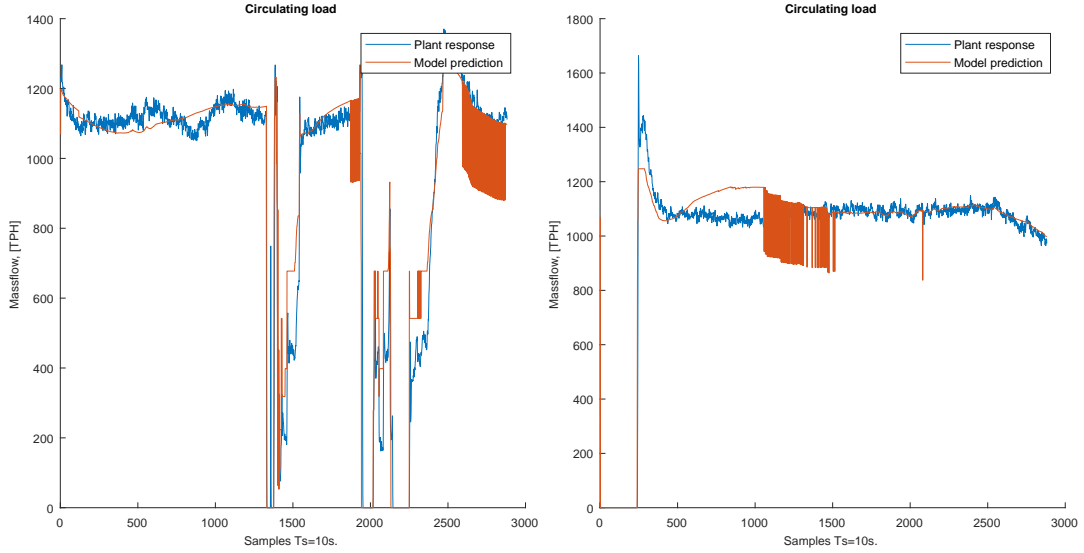
(d) validation set

Figure C.1: HPGR production, WIT402



(a) dataset 1

(b) dataset 2



(c) dataset 3

(d) validation set

Figure C.2: Circulating load, WIT416

C. Model calibration Figures

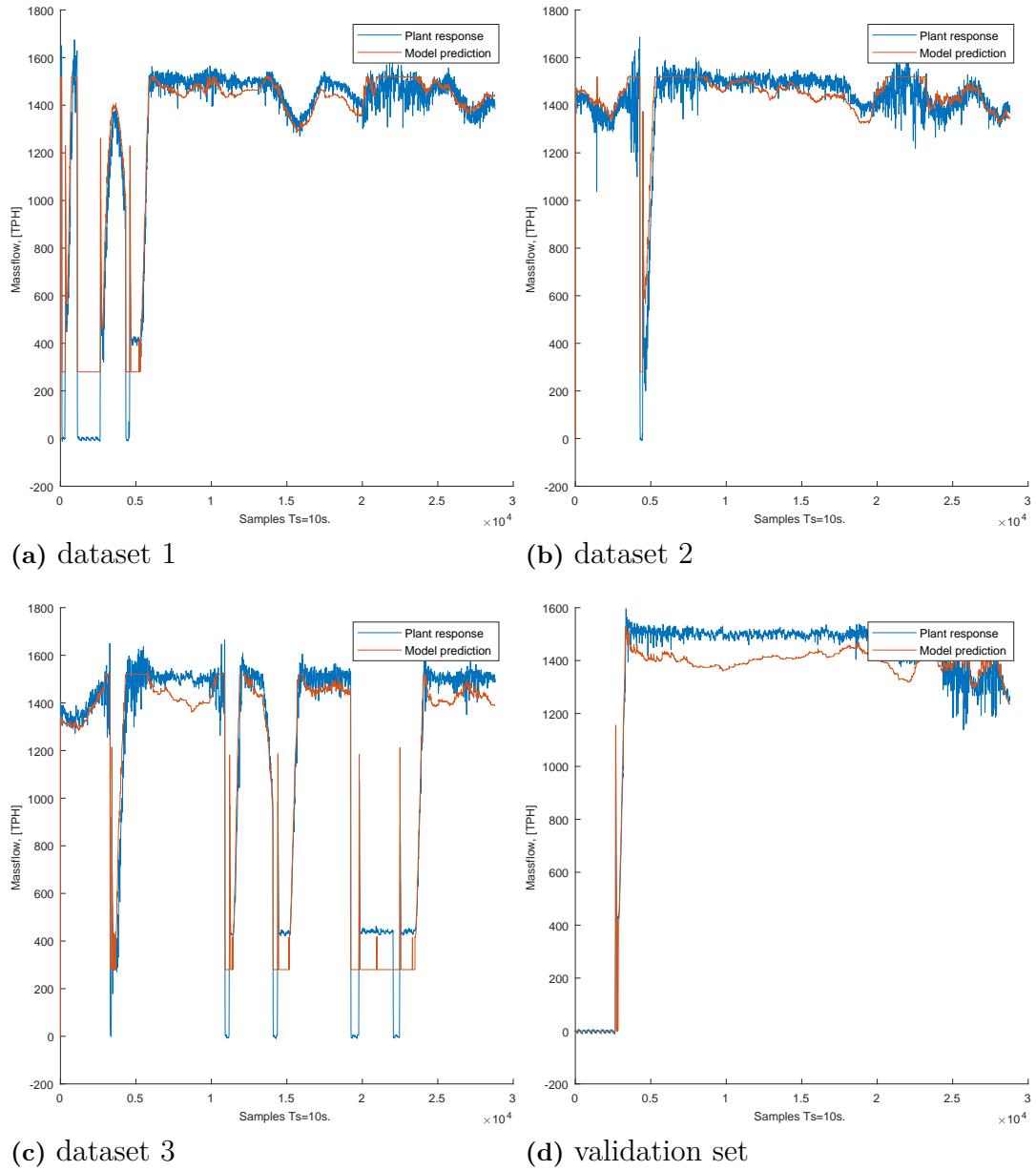


Figure C.3: Circuit inflow, WIT010B

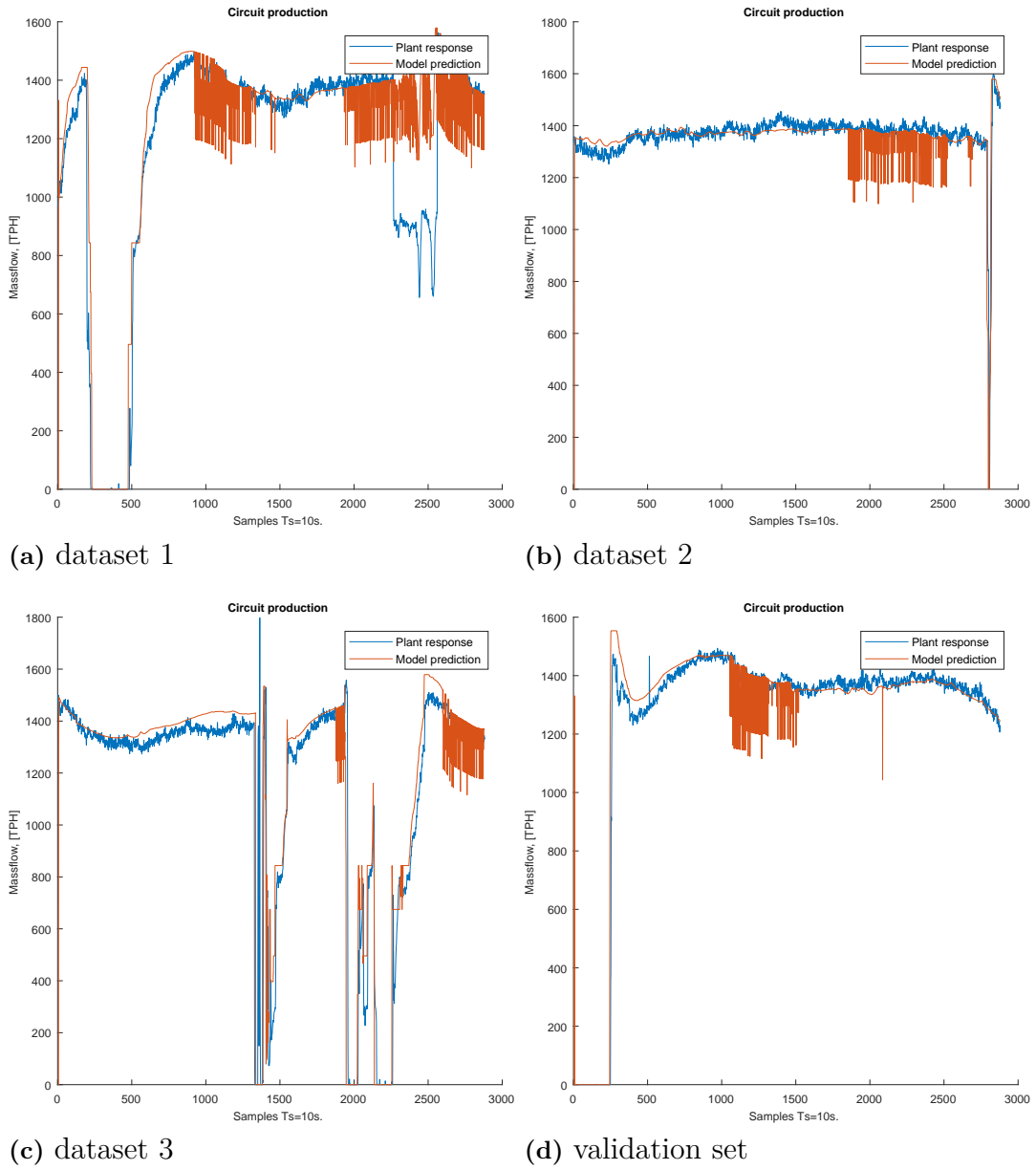


Figure C.4: Circuit output, WIT433

C. Model calibration Figures

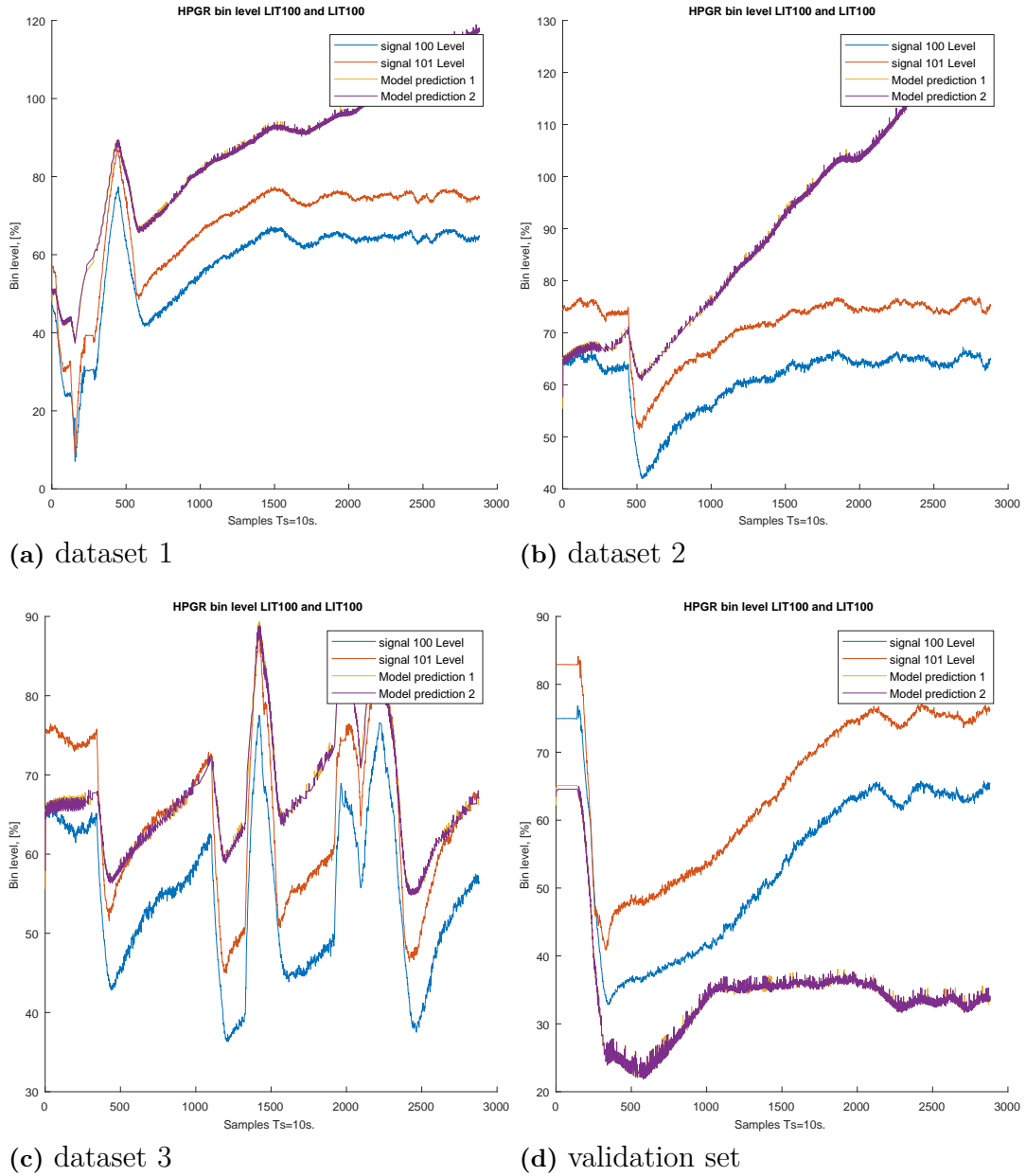


Figure C.5: HPGR-bin level, LIT100/101

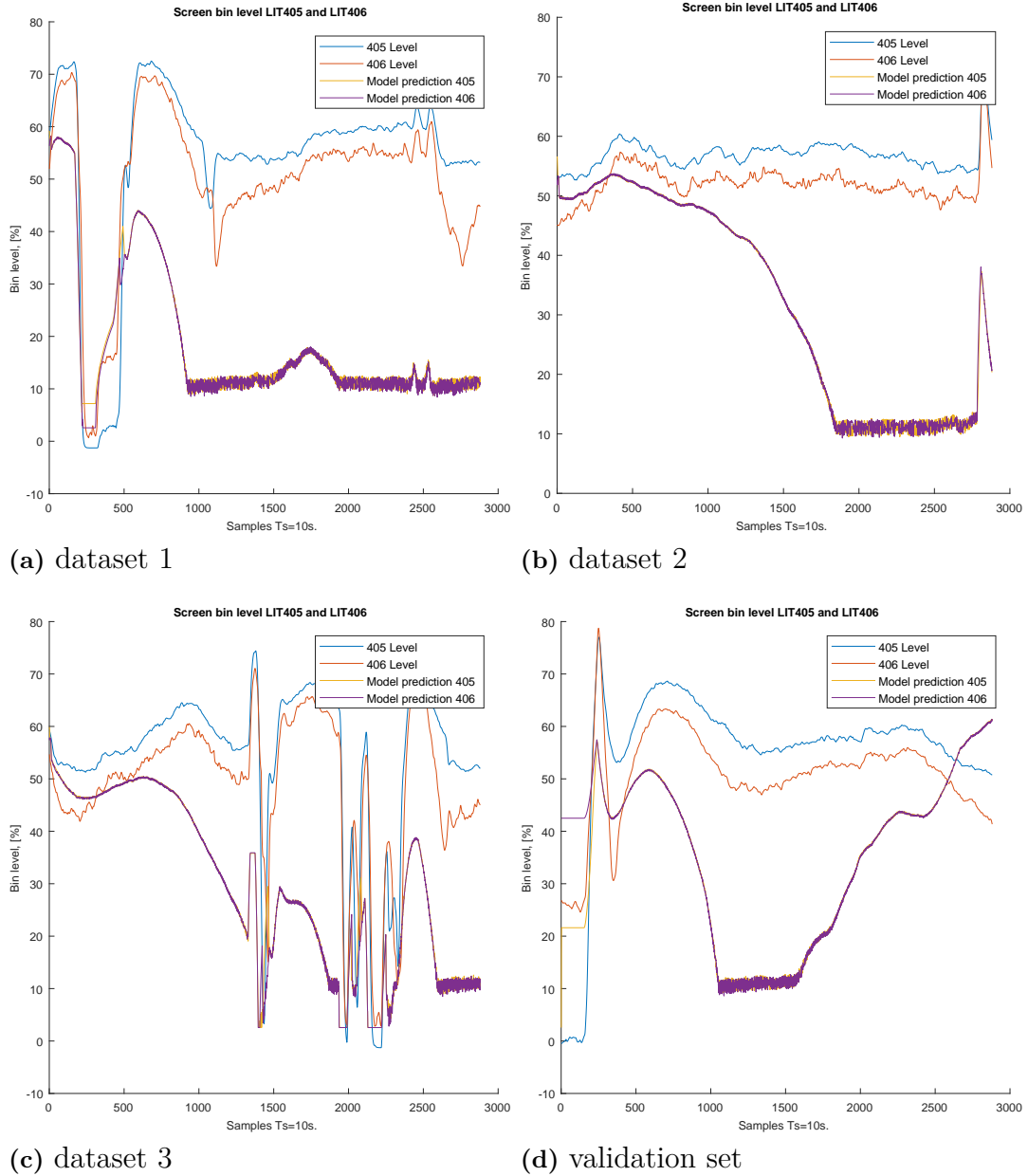


Figure C.6: Screen-bin level, LIT405/406

C. Model calibration Figures

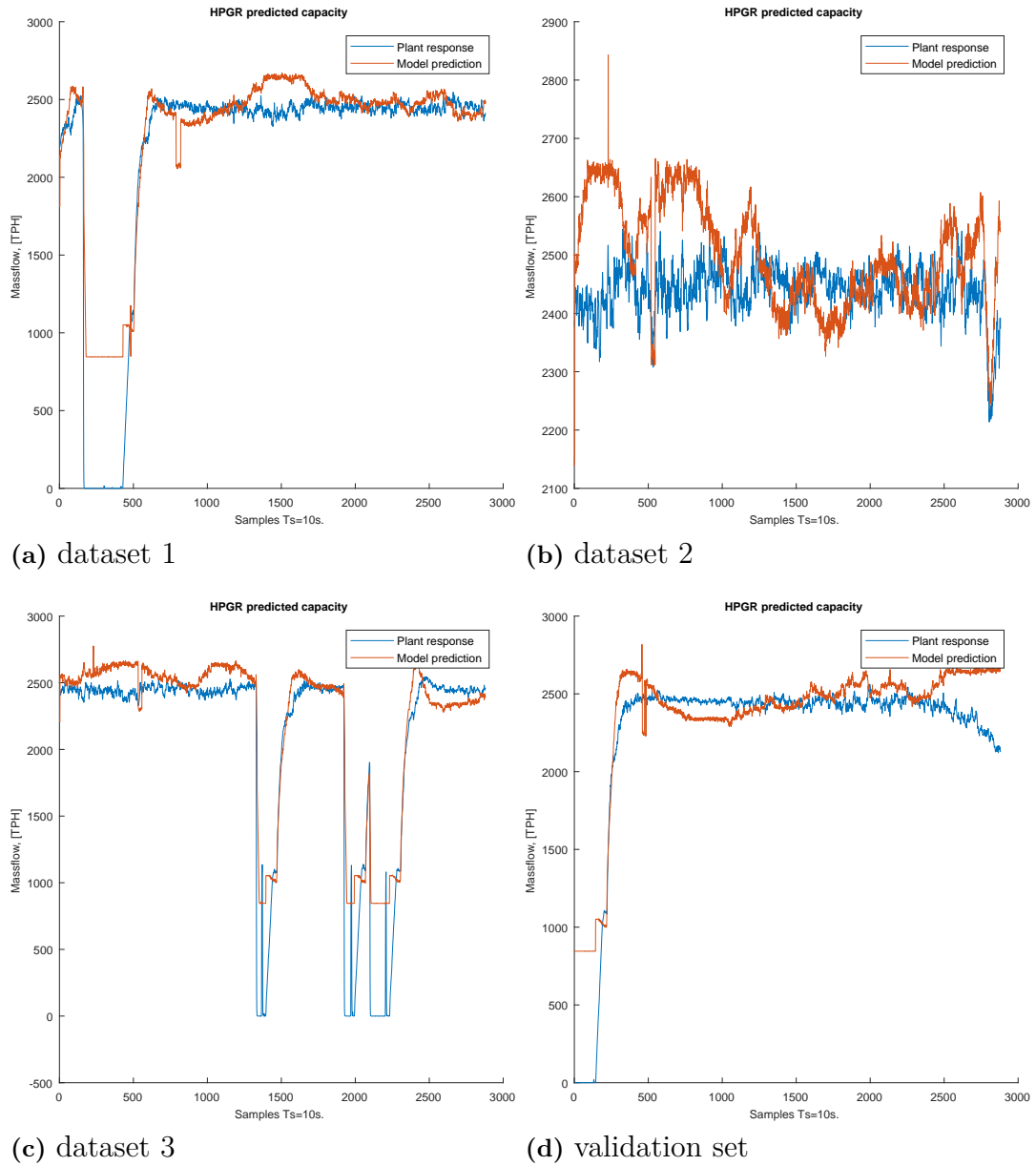


Figure C.7: HPGR predicted capacity

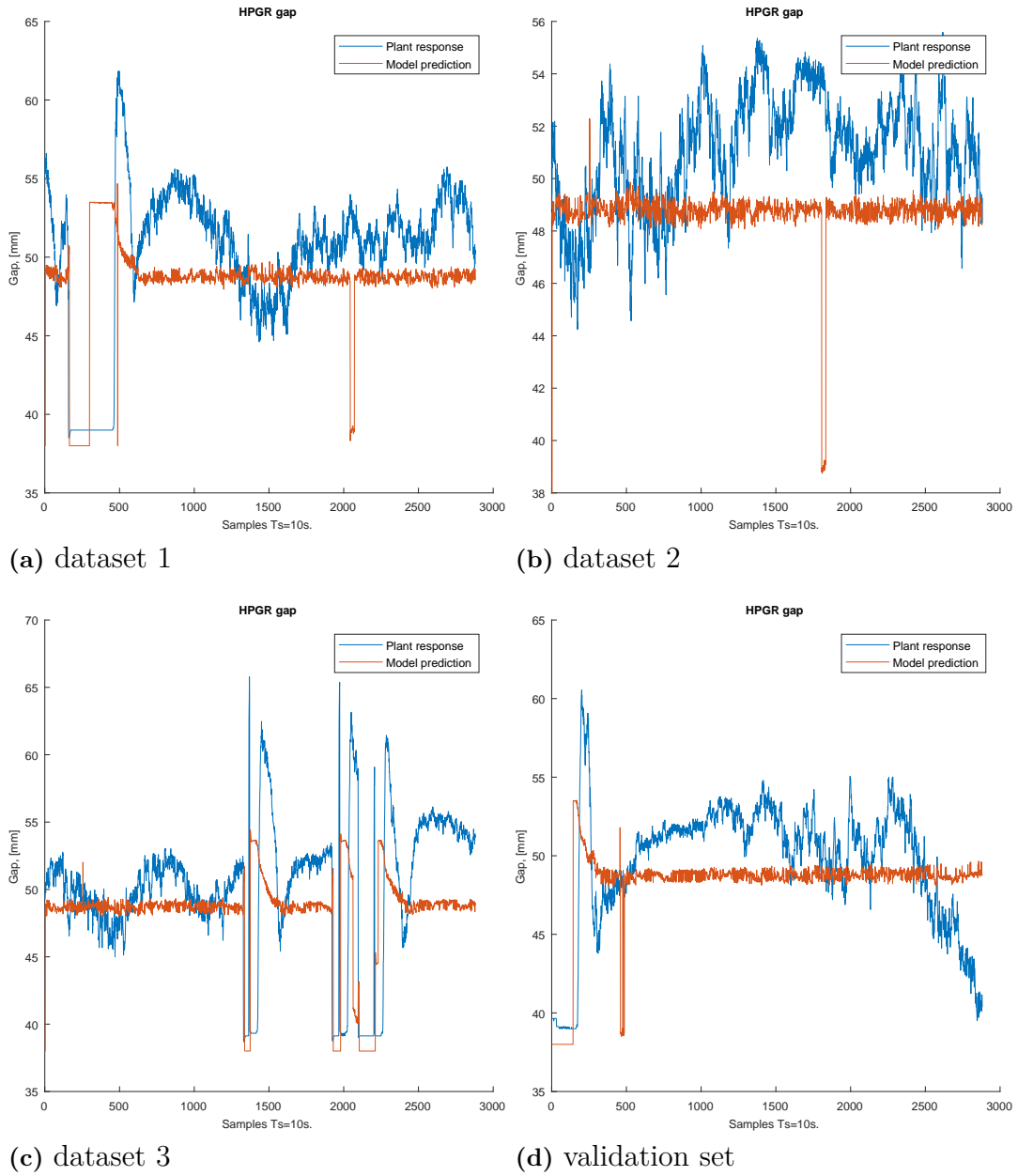


Figure C.8: HPGR operating Gap

D

Process layouts

D.1 Process layout illustrations

The three illustrations of the process, including the plain process, one with the SISO loops printed out and one with the MPC- state space model.

D. Process layouts

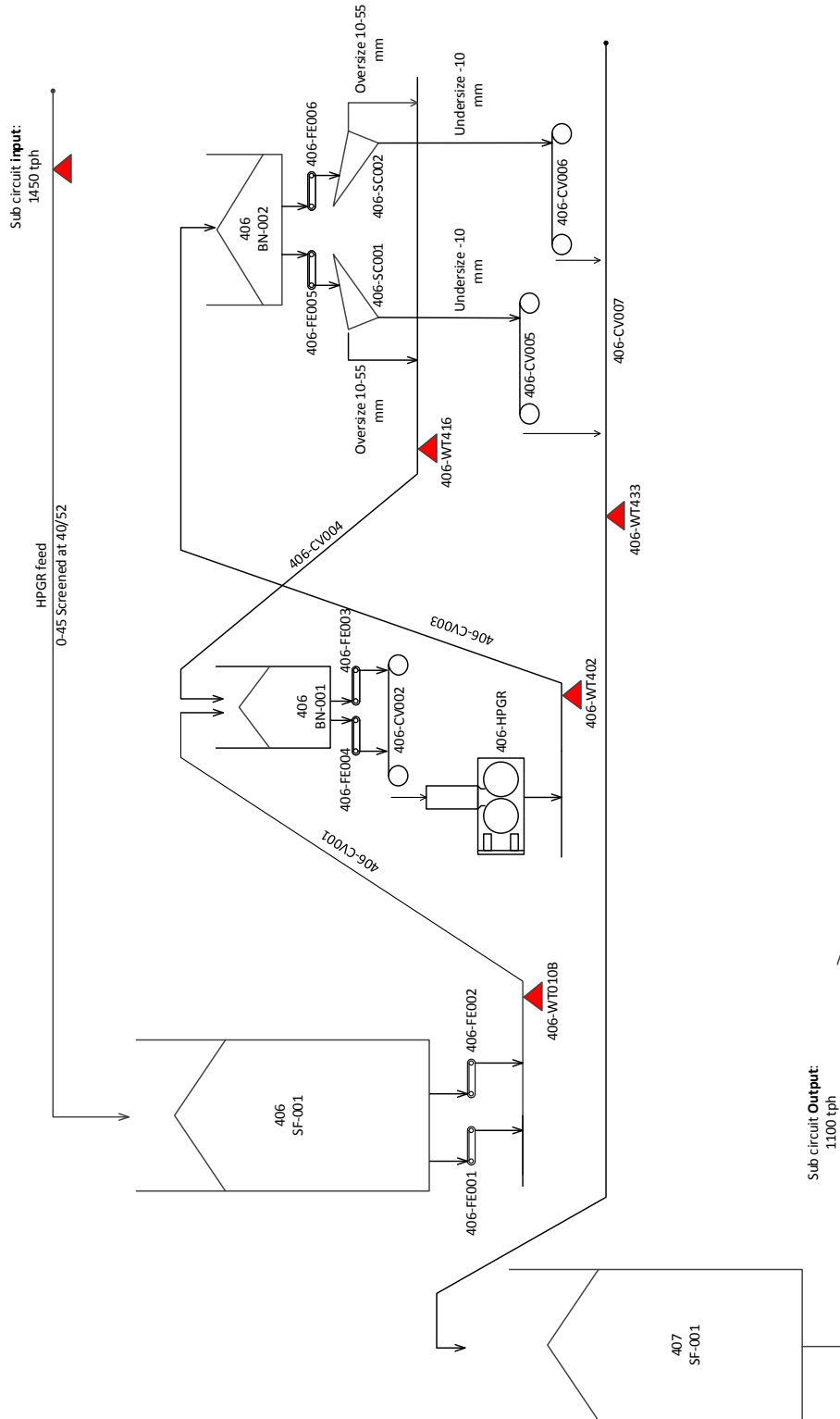


Figure D.1: Section 406 at Mogalakwena North.

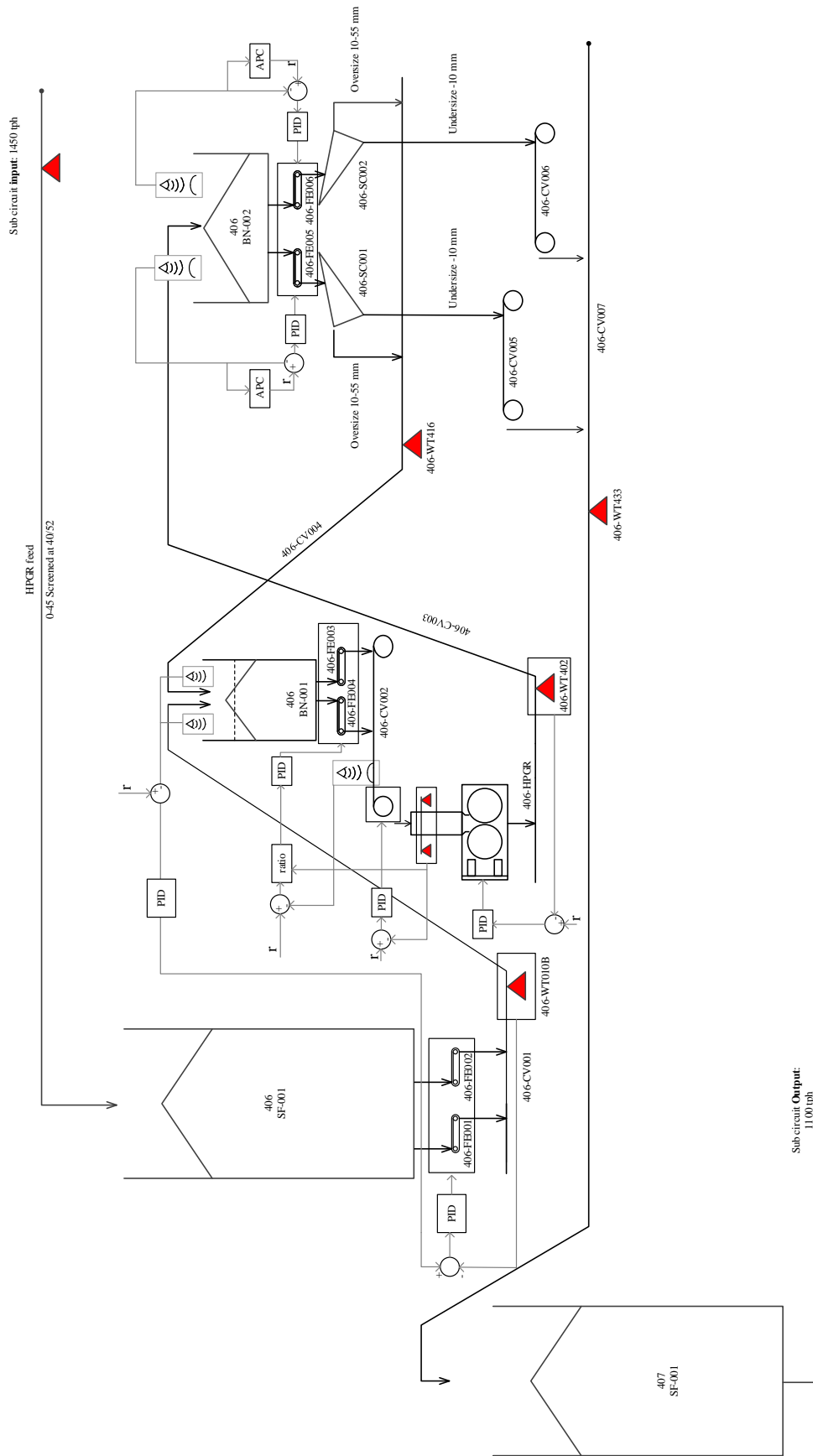


Figure D.2: SISO loops on section 406 at Mogalakwena North.

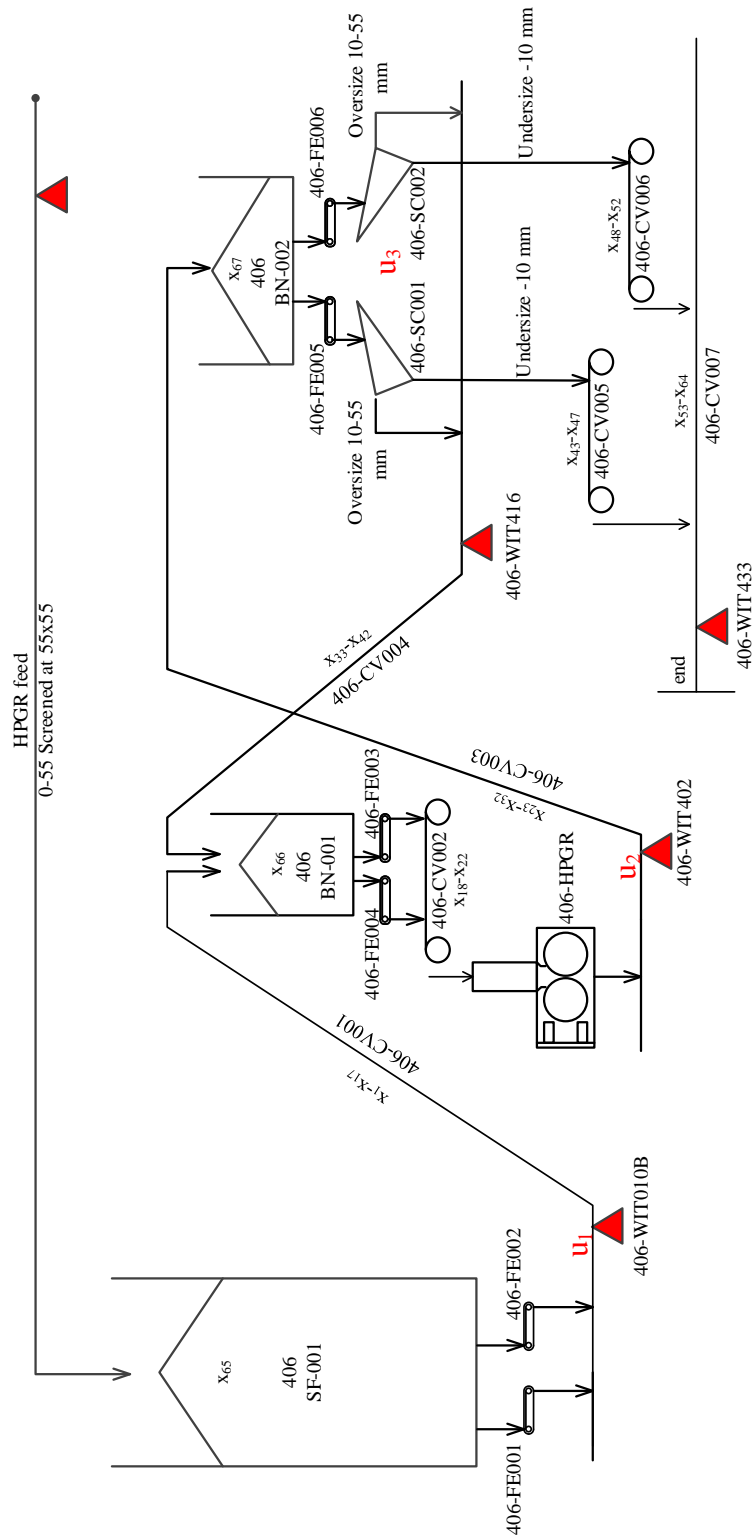


Figure D.3: The control model used in the MPC controller.